

**PROBABILISTIC SEISMIC RISK ASSESSMENT ON A MODEL
HOSPITAL**

A

PROJECT REPORT

Submitted in partial fulfilment of the requirements for the award of the degree of

BACHELOR OF TECHNOLOGY

IN

CIVIL ENGINEERING

Under the supervision

of

Dr. Sugandha Singh

(Assistant Professor)

By

Rada Wangmo (191628)

Tenzin Wangchuk (191629)

To



JAYPEE UNIVERSITY OF INFORMATION TECHNOLOGY

WAKNAGHAT SOLAN-173234

HIMACHAL PRADESH INDIA

May, 2023

DECLARATION

I hereby declare that the work presented in the Project report entitled “**PROBABILISTIC SEISMIC RISK ASSESSMENT ON A MODEL HOSPITAL**” submitted in partial fulfillment of the requirements for the degree of Bachelor of Technology in Civil Engineering at **Jaypee University of Information Technology, Wagnaghat** is an authentic record of my work carried out under the supervision of **Dr. Sugandha Singh**. This work has not been submitted elsewhere for the reward of any other degree/diploma. I am fully responsible for the contents of my project report.

Rada Wangmo (191628)
Department of Civil Engineering
Jaypee University of Information Technology,
Wagnaghat, India.

Tenzin Wangchuk (191629)
Department of Civil Engineering
Jaypee University of Information Technology,
Wagnaghat, India

CERTIFICATE

This is to certify that the work which is being presented in the project report titled **“PROBABILISTIC SEISMIC RISK ASSESSMENT ON A MODEL HOSPITAL”** in partial fulfillment of the requirements for the award of the degree of Bachelor of Technology in Civil Engineering submitted to the Department of Civil Engineering, **Jaypee University of Information Technology, Wagnaghat** is an authentic record of work carried out by **Rada Wangmo (191628) and Tenzin Wangchuk (191629)** during a period from July 2022 to May, 2023 under the supervision of **Dr. Sugandha Singh** (Assistant Professor), Department of Civil Engineering, Jaypee University of Information Technology, Wagnaghat.

The above statement made is correct to the best of our knowledge.

Date:

Dr. Sugandha Singh
Assistant Professor
Department of Civil Engineering
JUIT, Wagnaghat

Prof. (Dr.) Ashish Kumar
Professor & Head of Department
Department of Civil Engineering
JUIT, Wagnaghat

ACKNOWLEDGEMENT

To begin with, we want to show appreciation to the divine Kencho-Sum (The Triple Gem) for continuously keeping us healthy and mentally prepared to continue this project. We are grateful and indebted for the protection of Mahakala, the Buddhist Protector Deity, and we hope our faith will keep us grounded and humble.

We would like to give special thanks to our project mentor, Dr. Sugandha Singh, who provided us with valuable guidance, encouragement, and support throughout the entire project. Her expertise and insightful feedback were crucial in keeping us on track and helping us successfully complete the project. We also want to thank the Civil Engineering Department faculty at Jaypee University of Information Technology for providing us with a strong academic foundation and the necessary knowledge and skills to undertake this project.

Furthermore, we are grateful to the staff and management of Jaypee University of Information Technology for allowing us to use their resources and facilities to conduct our project work. Their cooperation and support made it possible for us to complete the project within the given timeline and learn more about earthquake and disaster assessment.

We also want to acknowledge the contribution of our colleagues and friends who supported us throughout the project, provided their insights and suggestions, and helped us overcome various challenges.

Finally, we want to express our heartfelt thanks to our family for their unwavering support and encouragement throughout our academic journey. Their love, motivation, and blessings played an instrumental role in keeping us focused and motivated.

Once again, we want to extend our sincere thanks to everyone who contributed to the completion of this project. Without your support, we would not have achieved this accomplishment

ABSTRACT

Earthquakes have always posed a danger to human life and been a significant source of infrastructure damage. The major purpose of healthcare institutions is to save lives and lessen the effects of disasters; yet previous earthquakes have caused physical damage, jeopardized lives and ruined such facilities and other such important buildings. Hospital resilience (i.e., endurance and structural rigidity) has always been crucial, but in the past few years, emphasis has been set exclusively on this issue, particularly in the wake of the World Health Organization's (WHO, 2008) and United Nations International Strategy for Disaster Reduction's (UNISDR) global campaign '*Hospitals Safe From Disasters*'; the World Health Day (7 April 2009) and the International Day for Disaster Reduction's (14 October 2009) world campaigns. "*There are countless examples of health infrastructure — from sophisticated hospitals to small but vital health centre — that have suffered this fate. One such case occurred in the Hospital Juarez in Mexico. In 1985, almost 600 patients and staff lost their lives when this modern (for its time) and well equipped hospital collapsed in the wake of an earthquake*" (WHO, 2007a).

Evidence from literature and practical experience indicate that healthcare interruptions are frequent after earthquakes, although the reasons for these interruptions are not entirely obvious. The current study goes over the physical damages (post-earthquake) to various hospitals, their impacts, and an analysis of the pre-earthquake risks evaluation on a model hospital by utilizing seismic probabilistic approach.

Probabilistic Seismic Hazard Analysis (PSHA) is used to forecast upcoming earthquake occurrences at a specific location in order to prevent or prepare for all this harm. PSHA seeks to quantify the probability (or rate) of surpassing different ground-motion levels at a site (or map of sites) given all potential earthquakes. PSHA produces a Uniform Hazard Spectrum (UHS), which is then used to do a Probabilistic Seismic Risk Assessment (PSRA), which compares the likelihood that a structure would fail to a seismic parameter like the peak ground acceleration of the ground motion.

Keywords: Probabilistic Seismic Hazard Analysis (PSHA), Uniform Hazard Spectrum (UHS), Probabilistic Seismic Risk Assessment (PSRA), Peak Ground Acceleration (PGA)

List of Figure

Figure 1 During an earthquake.....	1
Figure 2 Seismic Waves	2
Figure 3 Bhuj Earthquake.....	3
Figure 4 1971 Earthquake Damage of Olive View Hospital.....	6
Figure 5 Collapse of Juarez Hospital.....	7
Figure 6 Non-structural components.....	8
Figure 7 Damage to water supply pipes in Ridgecrest healthcare facility.....	8
Figure 8 1923 Great Kanto Earthquake	9
Figure 9 Erzincan Earthquake, Turkey	11
Figure 10 PSRA methodology	13
Figure 11 Contour Map of USA.....	18
Figure 12 Global Seismic Hazard Map	19
Figure 13 PSHA Procedure	20
Figure 14 Schematic illustration of the basic five.....	21
Figure 15 Schematic illustration of the basic five steps in PSHA	22
Figure 16 Typical distribution of observed earthquake magnitude	25
Figure 17 Campbell and Joyner & Boore Ground Motion Prediction Equations	28
Figure 18 PGA graph.....	28
Figure 19 Source to site distance.....	29
Figure 20 Slip Terminology	31
Figure 21 GMPE and M-R	33
Figure 22 PGA to Distance Graph.....	33
Figure 23 Probability of exceedence	34
Figure 24 Hazard Curve	34
Figure 25 Soil Profile of Takahagi.....	37
Figure 26 Peak Acceleration Contour Map of Japan	38
Figure 27 Strong Motion Data	39
Figure 28 Spectral Data of GM with 2 frequencies.....	39
Figure 29 G+2 Hospital Model.....	40
Figure 30 G+2 Hospital Model.....	40
Figure 31 Applying Eigen Value.....	42
Figure 32 Spectral Data for the Time History Analysis	42
Figure 33 GM1 THA 0.2g	43
Figure 34 GM1 THA 1g	43
Figure 35 GM1 THA 0.4g	44
Figure 36 GM1 THA 0.3g	44
Figure 37 GM1 THA 0.6g	45
Figure 38 GM1 THA 0.5g	45
Figure 39 GM1 THA 0.8g	46

Figure 40 GM1 THA 0.7g	46
Figure 41 GM1 THA 1g	47
Figure 42 GM1 THA 0.9g	47
Figure 43 GM2 THA 0.1g to GM2 THA 1g	48
Figure 44 GM1 Response Spectrum	49
Figure 45 GM2 Response Spectrum	50
Figure 46 Spectral Data for the Time History load case	51
Figure 47 Adding ground acceleration data like arrival time and scale factor	52
Figure 48 Performing Analysis	52
Figure 49 Result.....	53
Figure 50 Applying the dead load and live load scale factor.....	54
Figure 51 Extracting the Results from other spectral Acceleration Data.....	54
Figure 52 Analysing Drift Result	55
Figure 53 Drift Result	55
Figure 54 GM2: at 0.8g, G and G+1 storey failed.	55
Figure 55 GM1: at 0.7g, G and G+1 storey failed.	55
Figure 56 Fragility Curve for G+2	56

LIST OF TABLES

Table 1 Case Study on Erzincan Earthquake.....	10
Table 2 Faulting Mechanism	30
Table 3 Building Code Site classes	31
Table 4 Soil Condition Data for TAKAHAGI	36

TABLE OF CONTENT

CHAPTER 1: INTRODUCTION	1
1. BACKGROUND	1
1.1 EARTHQUAKES.	1
1.12 DIFFERENT TYPE OF EARTHQUAKE WAVES	2
1.2 HISTORY	2
1.3 EARTHQUAKE RESPONSE MEASURES	3
1.4 SUMMARY	4
CHAPTER 2: LITERATURE REVIEW	5
1. GENERAL	5
2. STRUCTURAL FAILURE	5
2.11 COLUMN FAILURE	6
2.12 BEAM FAILURE	7
2.2 NON-STRUCTURAL FAILURE	7
2.21 WATER PIPE FAILURE	8
2.22 ELECTRICAL CIRCUIT FAILURE	9
2.3 CASE STUDY ON ERZINCAN EARTHQUAKE	10
2.3 HYPOTHESIS	11
CHAPTER 3	12
METHODOLOGY	12
3.1 RUNNING THE OPENQUAKE ENGINE	14
CHAPTER 4	17
1. PROBABILISTIC SEISMIC HAZARD ASSESSMENT (PSHA)	17
2. PROBABILISTIC SEISMIC HAZARD ANALYSIS	17
KEY ASSUMPTIONS IN CALCULATING PROBABILISTIC GROUND MOTIONS	19
3. PSHA PROCEDURE – OBJECTIVE	20
3.1 STEPS OF THE PROCEDURES	21
3.2 IDENTIFICATION OF SEISMIC SOURCES	23

3.3 QUANTIFYING THE SEISMICITY RATE OF SOURCES (THE DEVELOPMENT OF MAGNITUDE- RECURRENCE RELATIONSHIPS FOR ALL SOURCES).	23
3.4 THE SELECTION OF ATTENUATION MODEL (OR GROUND MOTION PREDICTION EQUATIONS, GMPES)	25
3.4.1 ATTENUATION RELATIONSHIPS	26
3.4.2 RANDOM ERROR OF ATTENUATION MODEL.	28
3.4.3 SOURCE TO SITE DISTANCE	29
3.4.4 FAULTING MECHANISM	30
3.4.5 SLIP TERMINOLOGY	31
4. GROUND MOTION INTENSITY	32
5. THE DEVELOPMENT OF HAZARD CURVES FOR THE SITES.	32
6. SITE AMPLIFICATION ANALYSIS	35
7. PROBABILISTIC SEISMIC RISK ASSESSMENT	35
CHAPTER 5	36
DATA COLLECTION AND ANALYSIS	36
1. SITE LOCATION	36
1. DATA COLLECTION	39
2. ANALYSIS OF G+2 STRUCTURAL MODEL OF A HOSPITAL ON MIDAS GEN 2021	40
3. PERFORMING TIME HISTORY ANALYSIS	40
1. RESULT	53
2. ANALYSE THE RESULT.	55
CHAPTER 6	57
CONCLUSION & RECOMMENDATIONS	57
CONCLUSION	57
RECOMMENDATIONS	58

CHAPTER 1: INTRODUCTION

1. BACKGROUND

1.1 EARTHQUAKES.

An earthquake occurs when there is a sudden release of tension energy in the Earth's crust, which causes tremor waves to radiate outward from the epicenter. When stresses in the crust are greater than the maximum allowable strength of the rock, the rock cracks along weak points, either an old or new fault plane. An earthquake's focal point, or hypocenter, may lie many kilometres below the earth's surface.

The underlying idea of the elastic rebound theory is that before an earthquake, slow deformation is caused by tension that builds up in the rocks on each side of a fault. This deformation eventually overcomes the frictional force holding the rocks together, resulting in magnificent slip along the fault. As a result of the strain being released, the rocks on either side of the fault elastically rebound and revert to their original shapes, but offset

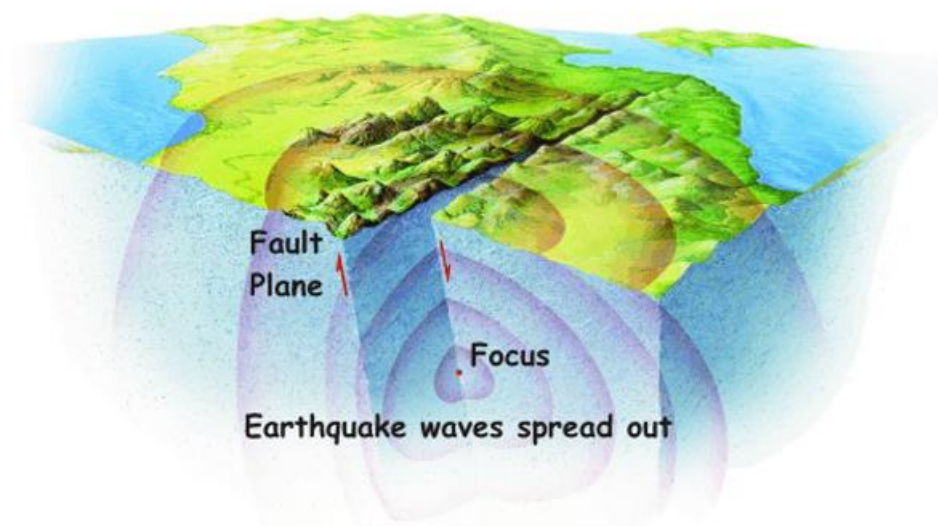


Figure 1 During an earthquake

1.12 Different type of Earthquake waves

After the introduction of seismology, a branch which deals with solely focus on the seismic waves, scientists have found different types of seismic waves through seismographs.

P waves, also known as primary waves, are the first waves that seismographs can detect since they are the quickest. These waves are compressional or longitudinal, pushing and pulling the earth parallel to the direction of the waves. Typically, they do very little harm.

S waves, also known as secondary waves, move more slowly than P waves. Although they move in the same direction, they shake the ground in a direction perpendicular to the wave's direction. Due to their greater amplitude, which causes a stronger vertical and horizontal motion of the ground surface, S waves are more hazardous than P waves.

Ground motion is produced by **Rayleigh waves** in both the vertical and horizontal directions. These waves have the potential to do the most damage since they pass by while elevating and lowering the earth.

Love waves oscillate horizontally.

1.2 HISTORY

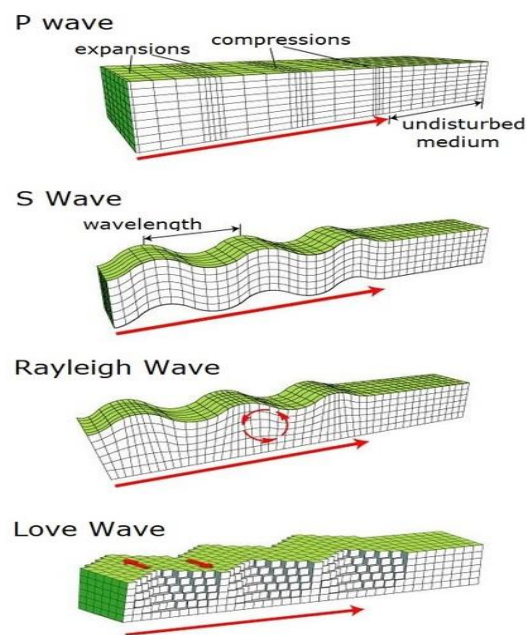


Figure 2 Seismic Waves

Earthquakes have wreaked havoc on everyday life throughout the past several decades, either by resulting in a large number of fatalities or in the damage of property. Landslides, tsunamis, surface liquefaction, and fire are also devastating earthquake aftereffects that produce more debris. Japan is the only country with a current example of how the 9.0 Richter scale Tohoku earthquake in 2011 caused a tsunami that wiped out coastal villages in the north pacific. In addition to an estimated 220 billion USD in property losses, it affected 602,200 inhabitants, killed 3.5% of them, and caused other damages. Japan's recovery from the disaster took around five years.

Even the Bhuj earthquake (magnitude 6.9 on Richter scale), 2001 in Gujarat, India resulted in nearly 20,000 deaths leaving half a million people homeless and an estimated loss of 10,000 crores.



Figure 3 Bhuj Earthquake

1.3 EARTHQUAKE RESPONSE MEASURES

With the advancement in geotechnical and earthquake engineering, researchers and experts have found and developed means to enhance resistance against such natural calamities. Even organisation like European Association for earthquake Engineering and PEER came into existence. Annual summits like World Conference on Earthquake Engineering are being held

to address earthquake related issues. For instance, the introduction of special provisions IS: 13920 was brought into the field to provide guidance in designing and building seismic resistant infrastructures. Another way is to make probabilistic assessments of the buildings against any odds like components, water pipes or equipment's malfunctioning which will or may result in eventual failure of the building during or after earthquake.

Upon focusing on such strategies, PSRA (probabilistic seismic risk assessment) was brought into limelight after having found to bring an honest result against safety earthquake measures. It basically focuses on the earthquake hazard assessment of the structures which may lead to certain risks in later stages by using statistical and probabilistic data analysing methods.

1.4 SUMMARY

Every now and then, an earthquake occurs about a certain region and the news of wreckage that follows it. Having to have heard and witness the dark history of earthquake incidents around the globe, it has now become vital to take measures to prevent such events from reoccurring. For that every structural engineers should be aware of the provisions that needs to be followed while designing and the concerned authorities to mandate the structural and non-structural assessment of the buildings periodically for any risk of failure.

Chapter 2: Literature Review

1. GENERAL

Even a small tremor can render a hospital unfunctional if its components are not properly monitored. The failure of a hospital during/ after an earthquake can be due to physical (structural and non-structural) or social (staff and administration) factors. The focus of this paper will be on physical attributes. *“The structural parts of a building are those that resist gravity, earthquakes, wind and other types of loads; they include columns; beams and foundations”*; and *“the non-structural parts include all parts of the building and its contents with the exception of the structure”*. *“They are composed of: lifeline facilities; medical facilities; and architectural elements”* (DoHS/WHO Nepal, 2004). Therefore all the malfunctioning due to elements like beam, columns, and walls are categorized under structural and architectural failure. The power cutoff, bursting of water failure, short circuiting and equipment failures in the hospital units are characterized as non-structural failure.

2. STRUCTURAL FAILURE

Hospital structural failures are frequently the result of poor detailing, irregular design, and poor selection of raw materials. Since non-structural components are typically connected to structures, which transfer earthquake forces onto them, structural behavior affects how they react (WHO SEARO, 2002). For instance, after the 1994 Northridge earthquake in the United States, the failure of St. John's Hospital's non-structural walls led to the bursting of water lines (Pickett, 1997); meanwhile, the Christian and Shiu-Tuan hospitals in Taiwan sustained only minor structural damage but significant utility and equipment damage during the 1999 Chi-Chi earthquake (Soong and Yao, 1999).

2.11 COLUMN FAILURE

One of the most crucial parts of an infrastructure is the column. In transferring axial compressive load from the top of the structure to the bottom footing, it is crucial. The newly constructed and earthquake-resistant Olive View Hospital was severely damaged to the point that it had to be eventually dismantled, according to the Design Implications of Damage Observed in Olive View Medical Centre Buildings during the 1971 San Fernando Earthquake report. The hospital's flooring were flat slabs with drop panels at the columns owing to how it was designed. Shear walls bound the wings from the second level to the roof. However, these stopped below, and the first and second floors were only supported by columns, creating what is known as a "soft-story" mechanism. Columns that were spirally strengthened and tied were used. The first two storeys sustained the majority of the damages: many of the linked columns broke and fell, and the spiral columns sustained significant spalling and cracking. The columns were damaged beyond repair, despite the fact that the structure did not collapse. The damage pattern showed that the structure underwent a significant inelastic deformation that was primarily in one direction.



Figure 4 1971 Earthquake Damage of Olive View Hospital

2.12 BEAM FAILURE

Beams are used to support the weight of the building's floors, ceilings and roofs by transferring the load to a vertically load-bearing component of the structure. Juarez Hospital completely fell apart as a result of the 1985 earthquake in Mexico City. In the Juarez Hospital's maternity wing, 400 medical personnel and patients were confined. This reinforced concrete frame structure collapsed due to localized failures at the beam-to-beam joints of each floor. Ten days after the earthquake, survivors were pulled from the building by tunneling through the rubble between the floor slabs.(Mexico City earthquake damage, September 19, 1985)



Figure 5 Collapse of Juarez Hospital

2.2 NON-STRUCTURAL FAILURE

The building's condition, the reliability of its utility sources, and the facility's regular operations are all important factors. The continuity of medical care is impacted when one or more of these parts fails.

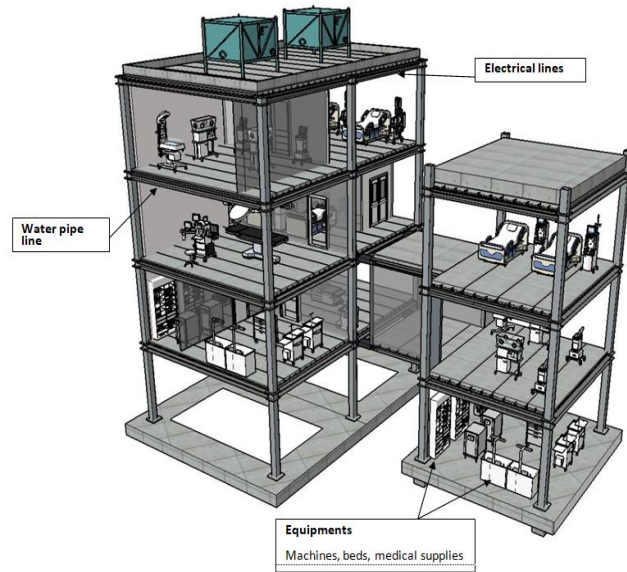


Figure 6 Non-structural components

2.21 Water Pipe Failure

The Ridgecrest healthcare center was rendered inoperable in 2019 by the Ridgecrest earthquake, which had a magnitude of 6.4. The building's structure was unaffected. However, a room packed with mechanical and electrical equipment flooded as a result of some leaky pipes, and water also entered the lift shafts and operating rooms. Hospital staff and patients were required to evacuate the building out of an abundance of caution (Ridgecrest Hospital's Quake Damage Prompts Questions About State Seismic Standards, CBS News).



Figure 7 Damage to water supply pipes in Ridgecrest healthcare facility.

2.22 Electrical Circuit Failure

The 7.9 magnitude Great Kanto Earthquake (1923), which had its epicentre a little more than 40 miles to the south-southwest of the capital of Japan, produced energy comparable to that of roughly 400 Hiroshima-size atomic bombs. The majority of the brick and unreinforced concrete structures in the Kant region collapsed after the initial shock, which lasted just over fourteen seconds. However, fire proved to be the most harmful to both people and Tokyo's actual built environment. Less than an hour after the earthquake, 130 different fires broke out in Tokyo, many of them were concentrated in the heavily populated eastern and north eastern wards of Asakusa, Nihonbashi, Kanda, Kybashi, Fukagawa, and Ginza.

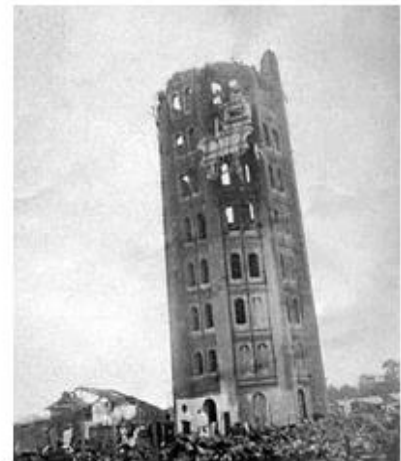


Figure 8 1923 Great Kanto Earthquake

2.3 Case Study on Erzincan Earthquake

Table 1 Case Study on Erzincan Earthquake

Date	Magnitude	Epicenter	Areas affected	Casualties
6 th Feb, 2023 (at 4:17am)	<ul style="list-style-type: none"> • First wave: 7.8 Ritcher scale • Aftershock: 7.5 	<ul style="list-style-type: none"> • Pazarcik district of Kahramanmaras Province 	<ul style="list-style-type: none"> • 10 provinces in Turkey • Lebanon • Syria • Cyprus • Iraq 	<ul style="list-style-type: none"> • Death: 45,986 death tolls (March 5th). • Financial: estimated material damage to reach 100 billion dollar. • Buildings: 214,577 buildings are identified as heavily damaged, demolished or in urgent need of demolition. • Facilities: Clean drinking water and food issues in Hatay.

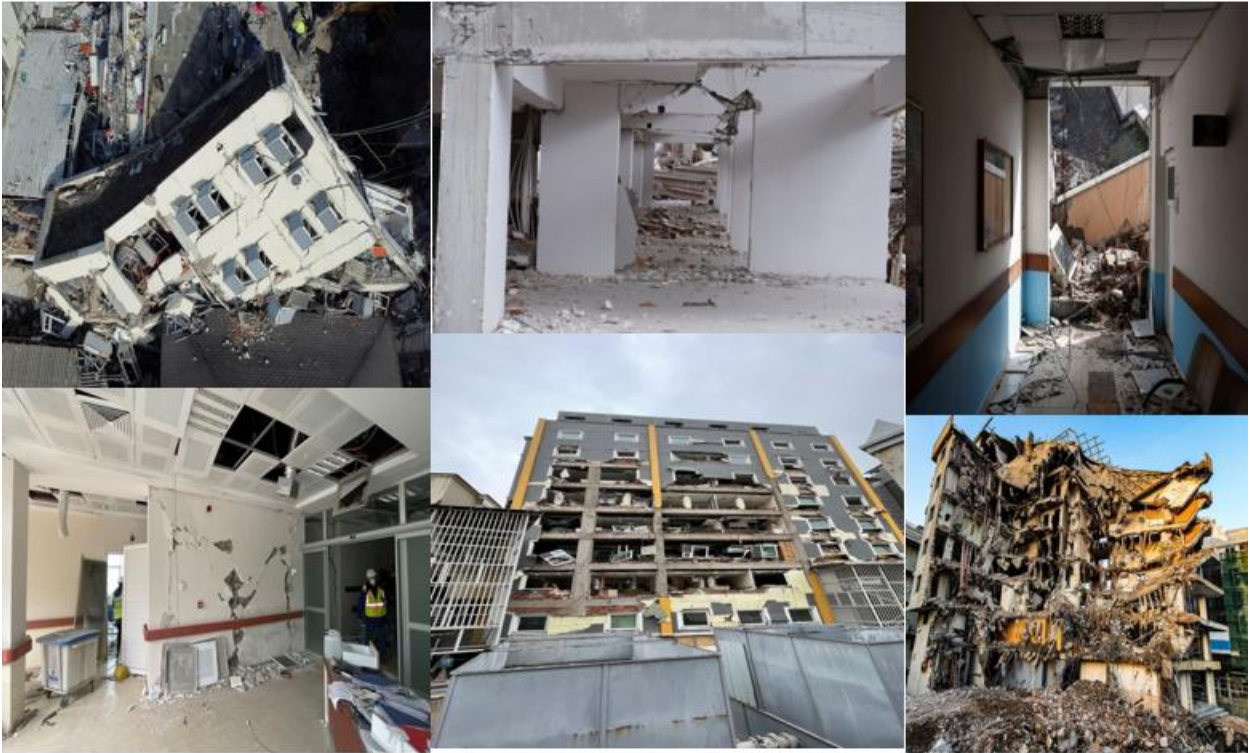


Figure 9 Erzincan Earthquake, Turkey

2.3 Hypothesis

If a seismic risk assessment is performed on a modelled hospital and the structural features are accurately modelled, while ensuring quality control measure are implemented for the building materials, then the hospitals ability to withstand earthquake induced stresses will be significantly increased, resulting in reduced risk of damage of collapse.

Chapter 3

Methodology

With the advancement in human knowledge in earthquake engineering, methods have been introduced to prevent or minimise loss and destruction during/after earthquake. One of such ways is called Probabilistic Seismic Risk Assessment (PSRA), which is an analytical process of understanding and predicting the response of a structure to an earthquake.

The quantification of the negative effect and the likelihood that it will occur over that time period are all included in a probabilistic seismic risk assessment, which estimates how an earthquake may affect people in the future.

Detailed models of the location, timing, and size distribution of earthquakes, as well as models of ground-motion attenuation with distance, are needed for accurate predictions of seismic hazard (and the related "risk" of social or economic repercussions). Modern probabilistic algorithms may be used to analyse this data to determine the amount of ground shaking danger, which is represented as the likelihood that one or more locations won't experience ground motion that exceeds a specific threshold during the time period of interest. The management of uncertainties resulting from insufficient information is made possible by the probabilistic techniques, which also offer a tested foundation for expressing natural variability.

1. Building information & Numerical models
 - Materials, Building type, design year, no. of stories, floor area, occupancy, etc.
 - Material capacities, FE modeling approach, simulated failure modes, infill strut model class, etc.

2. Probabilistic Seismic Hazard Analysis (PSHA)
 - Site seismic hazard curves for the selected Intensity Measure (IM)
 - Ground Motions (GMs) selection

For each model class

3. Probabilistic Seismic Demand Analysis (PSDA)
 Nonlinear Response History Analysis (NRHA) at selected IMs:
 - Engineering Demand Parameter
 - Building collapse fragility curve

4. Element damage & loss characterization
 - Damage functions for discrete Damage Measure (DM) levels
 - Loss functions for selected Decision Variables (DV)

5. Intensity-based probabilistic damage & loss analysis
 Building DV value for each IM value, as sum of elements seismic loss

6. Life-cycle probabilistic seismic loss analysis
 Life-cycle building DV value, as weighted sum of the different intensity levels contributions

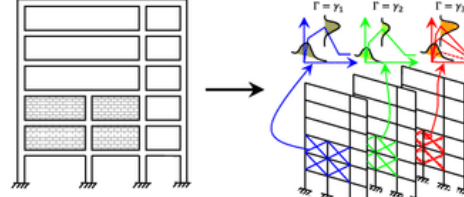
7. Weighted average time-based building seismic performance
 - Weighted average loss exceedance curve
 - Weighted average EAL value

$$v_{DV|\Gamma}(dv|\gamma) \cong \sum_{i=1}^{N_{IM}} [G_{DV|IM,\Gamma}(dv|im_i, \gamma) | \Delta v_{IM|\Gamma}(im_i|\gamma)]_i$$

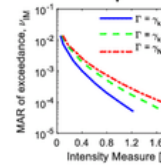
$$v_{DV}(dv) = \sum_{k=1}^{N_{class}} [v_{DV|\Gamma}(dv|\gamma_k)]_k P(\Gamma = \gamma_k)$$

$$EAL = \sum_{k=1}^{N_{class}} \left[\int_{dv} v_{DV|\Gamma}(dv|\gamma_k) d(dv) \right]_k P(\Gamma = \gamma_k)$$

1a. Case study building **1b. Numerical models: infill strut model classes**



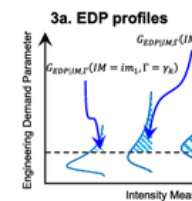
Site seismic map



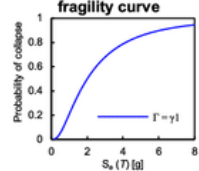
2. Seismic hazard curve

For each k model class

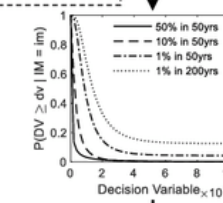
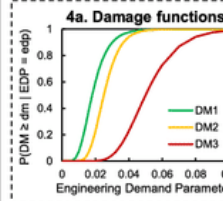
3. Model class PSDA



3b. Collapse fragility curve



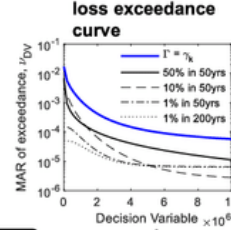
4. Element damage & loss characteristics



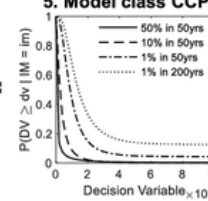
5. Model class Complementary Cumulative Performance Function (CCPF)

Repeat for all the N_{class} model classes

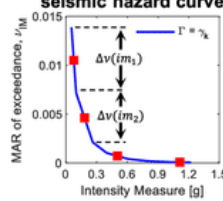
6. Model class loss exceedance curve



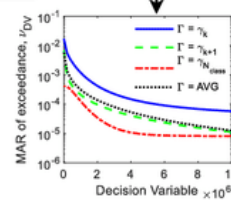
5. Model class CCPF



2. Model class seismic hazard curve



k = k+1



7. Weighted average loss exceedance curve

Figure 10 PSRA methodology

3.1 Running the OpenQuake Engine

PSHA is carried out using the OpenQuake programme (<https://openquake.org/>).

The environment of the OpenQuake Engine must be initialised before it can be used. The OpenQuake Engine (console) icon on the desktop or the 'Start' menu may both be double-clicked to do this. After being clicked, a command prompt will appear.

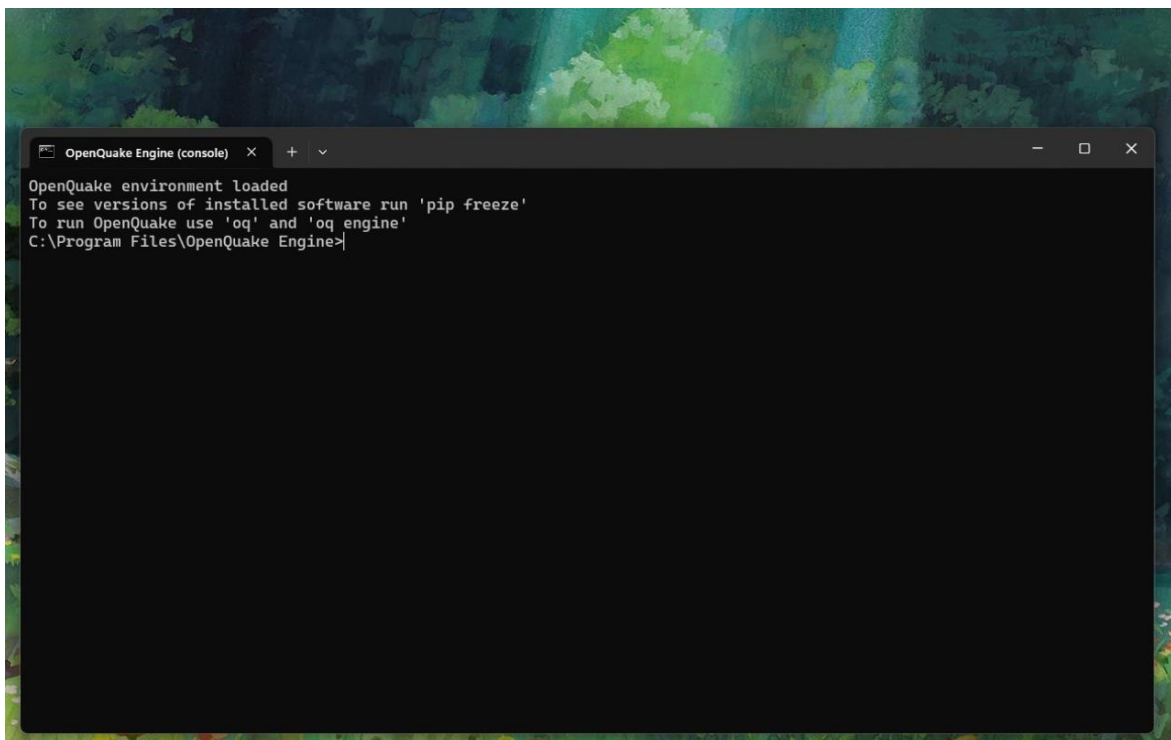


Figure OpenQuake Engine

Oq stands for OpenQuake Engine's command-line interface. The command oq engine must be launched in order to do a computation.

The package comes with a number of demonstration computations. The default location for them is C:\Program Files(x86)OpenQuake Engine\demos\\. The exact route could change depending on where the Engine has been installed.

3.2 Running via web interface (WebUI)

Double-clicking the OpenQuake Engine (webui) icon on the desktop or in the "Start" menu will activate and load the WebUI. There'll be a command window. The WebUI's address is <http://localhost:8800>, and a browser window will appear in a few seconds.

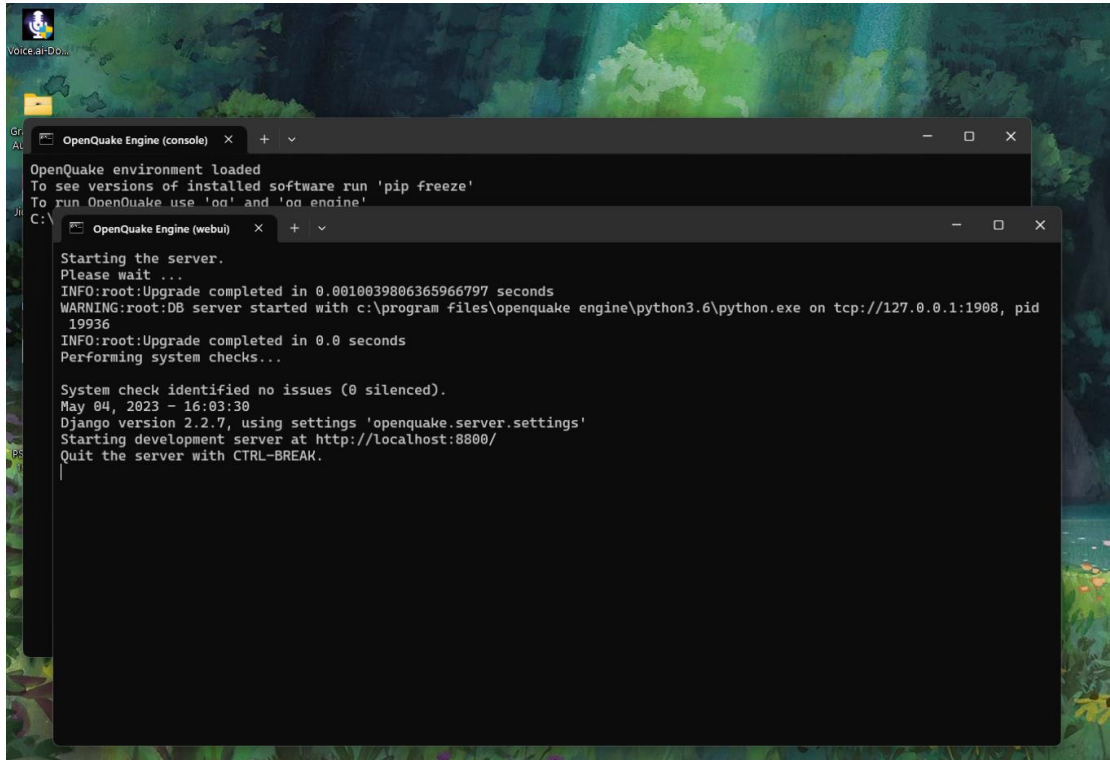


Figure OpenQuake

After a few seconds, OpenQuake Engine WebUI directs towards the web where the calculation needs to be done.

Once the command prompt appears, navigate to the directory where your OpenQuake input files are located by clicking Run a calculation. Once you are in the correct directory, you can run the OpenQuake Engine.

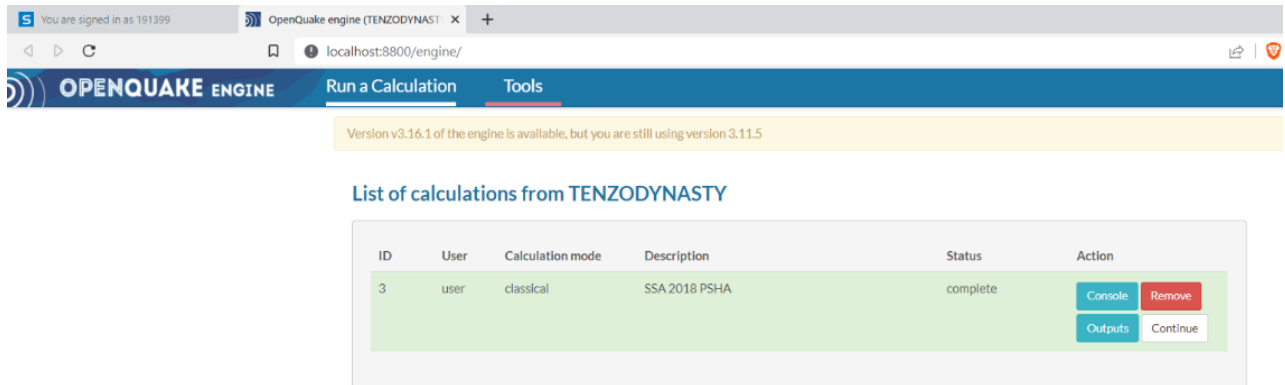


Figure OpenQuake WebUI

The OpenQuake Engine will now begin processing your input file. Depending on the size and complexity of your file, this may take some time.

Once the OpenQuake Engine has finished processing your file, the results will be displayed in the command prompt. You can also find the output files in the same directory as your input files.

The result Response Spectrum is used in the STAAD Pro to run the analysis.

CHAPTER 4

1. PROBABILISTIC SEISMIC HAZARD ASSESSMENT (PSHA)

The reason why probabilities are valuable in describing seismic hazard is due to the fact that earthquakes and their impacts are unpredictable events. Probabilistic seismic hazard analysis (PSHA) takes into consideration various factors, such as the varying seismic potential of different sources, the chance nature of earthquake events, the random nature of ground motion produced by earthquakes, the potential damage caused by these ground motions, and the uncertainties associated with every stage of the analysis.

PSHA is an all-inclusive approach that accounts for all possible causes, occurrences, and seismic sources as well as any uncertainties that could impact the seismic hazard results at a particular location. Before the widespread adoption of PSHA for assessing earthquake hazards, deterministic methods (DSHA) were commonly used, which were based on a single, most influential scenario.

2. Probabilistic Seismic Hazard Analysis

The approach of PSHA was originally developed by C.A. Cornell in 1968 and later it was modified by McGuire. Currently this method is also known as Cornell- McGuire methodology for hazard assessment. It was used by S.T. Algermissen et.al. (USGS) for developing a probabilistic seismic hazard map of US in 1976. And based on that hazard assessment results, the first or the most updated US seismic zone map was developed and was included in the then Uniform Building Code (US) in 1988. So since then this methodology is widely used and still currently widely used all over the world to perform the seismic hazard assessment and come up with seismic hazard map for any particular area or any particular site.

The figure below shows the results of seismic hazard assessment for US in 1976.

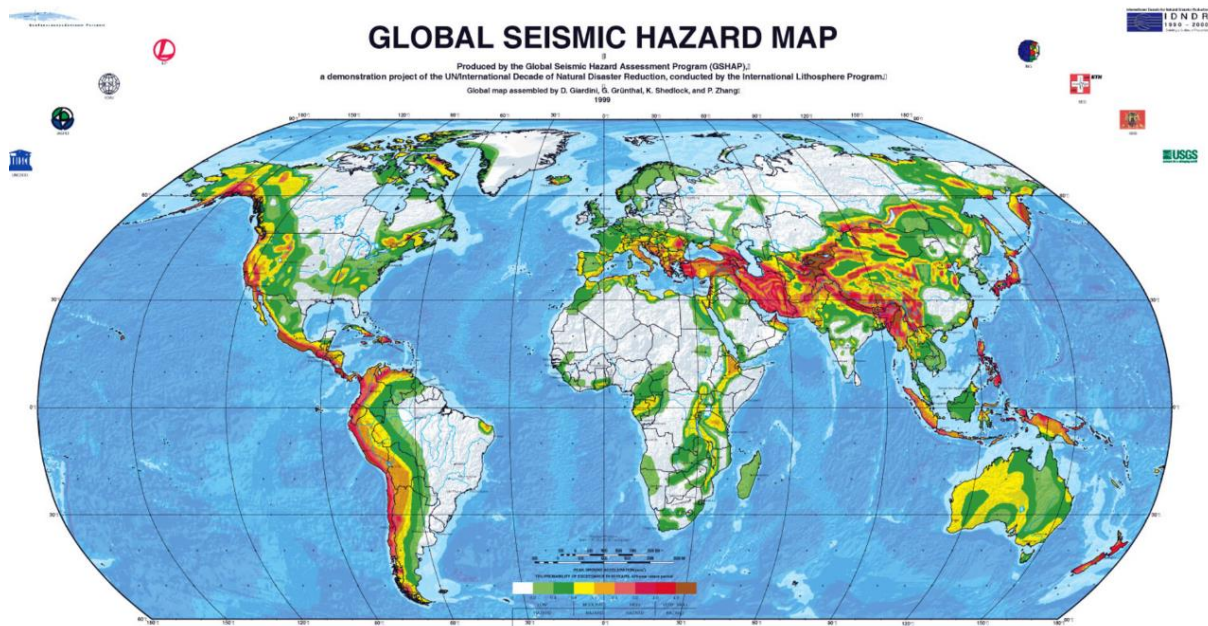


Figure 12 : Global Seismic Hazard Map

The global seismic hazard map developed by the project which is called Global Seismic Hazard Assessment Program (GSHAP), here we compare the relative seismic activity or seismic hazard for different countries or areas. The whole of the Himalayan Belt (India, Nepal, Bhutan and Pakistan) is high seismically active area. Similarly West Coast of North and South America, and Middle East Asia and Japan are High seismic active area.

Key Assumptions in Calculating Probabilistic Ground Motions

1. Within the specified seismic source zones or along the specified active faults, earthquakes happen.
2. Within any identified seismic source (or active fault), earthquakes can happen anywhere at any time with an equal risk of happening.
3. Earthquakes randomly occur throughout time inside each identified seismic source zone (or active fault), with the magnitude-recurrence relation defining the average rate of occurrences. A Poisson process is used to simulate this time-dependent random event.

4. According to statistics, there is no relationship between this earthquake's incidence and that of previous earthquakes.
5. With the aid of a chosen attenuation relationship (Ground Motion Prediction Equation (GMPE)), the ground motion parameter (for example, PGA, SA(spectral acceleration)) at the site of interest can be calculated for any earthquake event from the magnitude, source to site distance, and other earthquake parameters.

3. PSHA Procedure – Objective

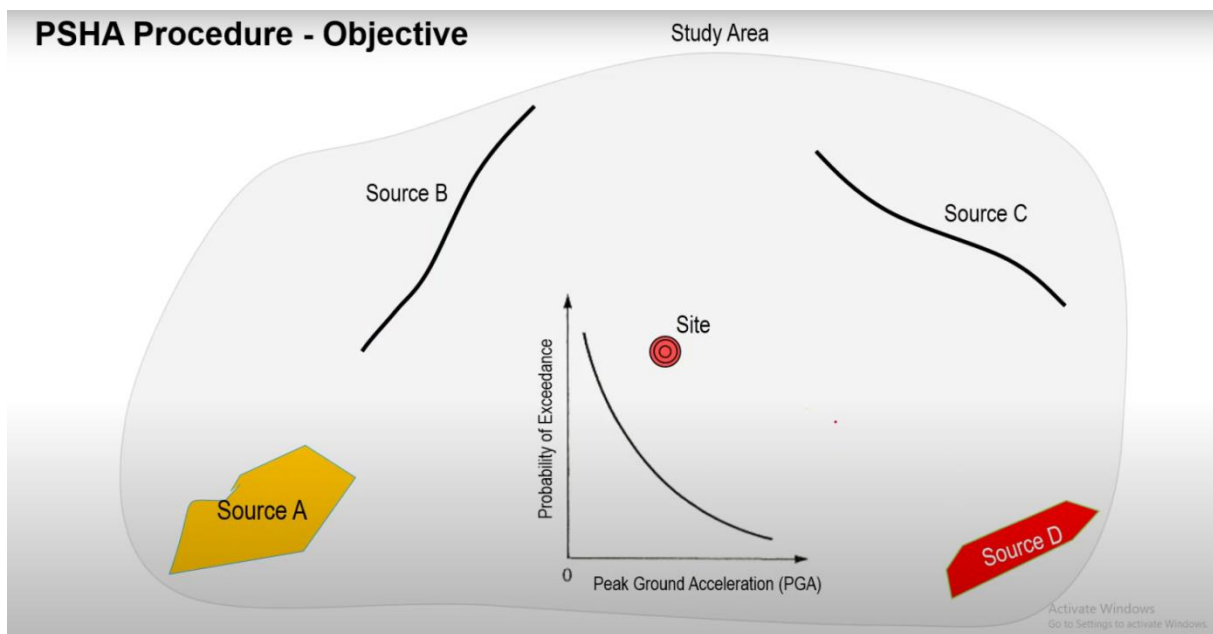


Figure 13 : PSHA Procedure

Now let's assume the above figure is our study area with several seismic sources. Assume that the source A is an area source and Historical data are available, and we don't understand the exact fault Geometry and orientation in this source. So we assume it as an area source. The source B is a fault which is a known fault and Source C is also a fault. Source D is an area source.

Using the historical data and the activity rate and the ground motion prediction equations, our target is to get Peak Ground Acceleration (PGA) at the site.

To calculate the PGA, PGA has to be linked with definition of hazard. We have to tell the probability of exceedance in some years. If we are able to do all the process for all the sources in the study area we can develop the seismic hazard map for this area.

3.1 Steps of the Procedures

- ✓ Select the site(s).
- ✓ Identification of all essential tectonic structures (such as active faults, seismic source zones, or sources local to an area, such as volcanoes), which are likely to produce large earthquakes.
- ✓ Defining the seismicity of these seismic sources (how active seismically that fault or source is). So we will quantify their seismic activity and that quantification will be based on past data.
- ✓ Once the quantification is done for all the seismic sources which can influence the hazard analysis than Selection of a suitable attenuation relationship is done (This equation calculates the ground motion parameters based on the magnitude of the earthquake and the source-to-site distance for various site circumstances.)
- ✓ Calculating the site's ground motion parameters.

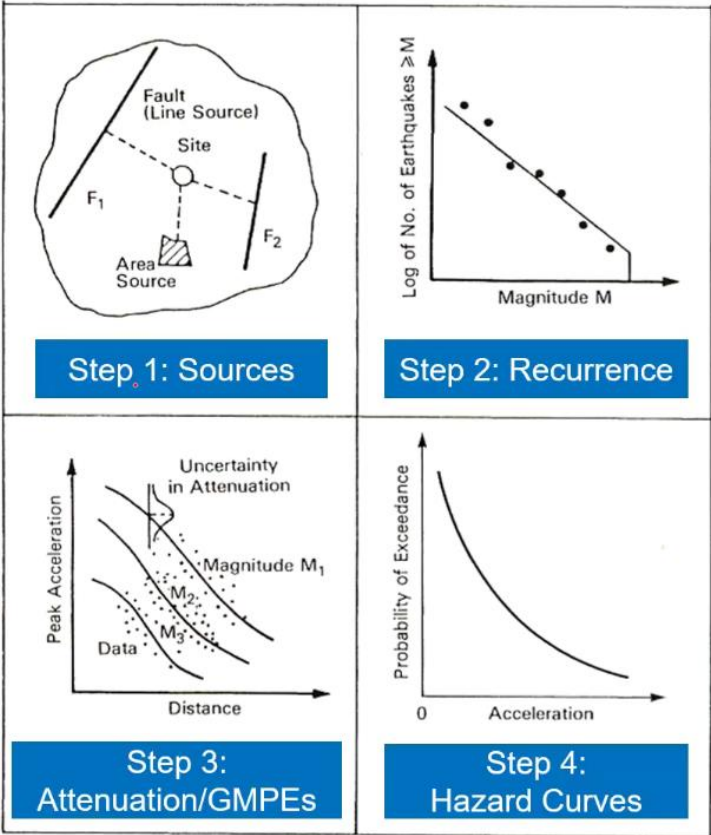


Figure 14: Schematic illustration of the basic five

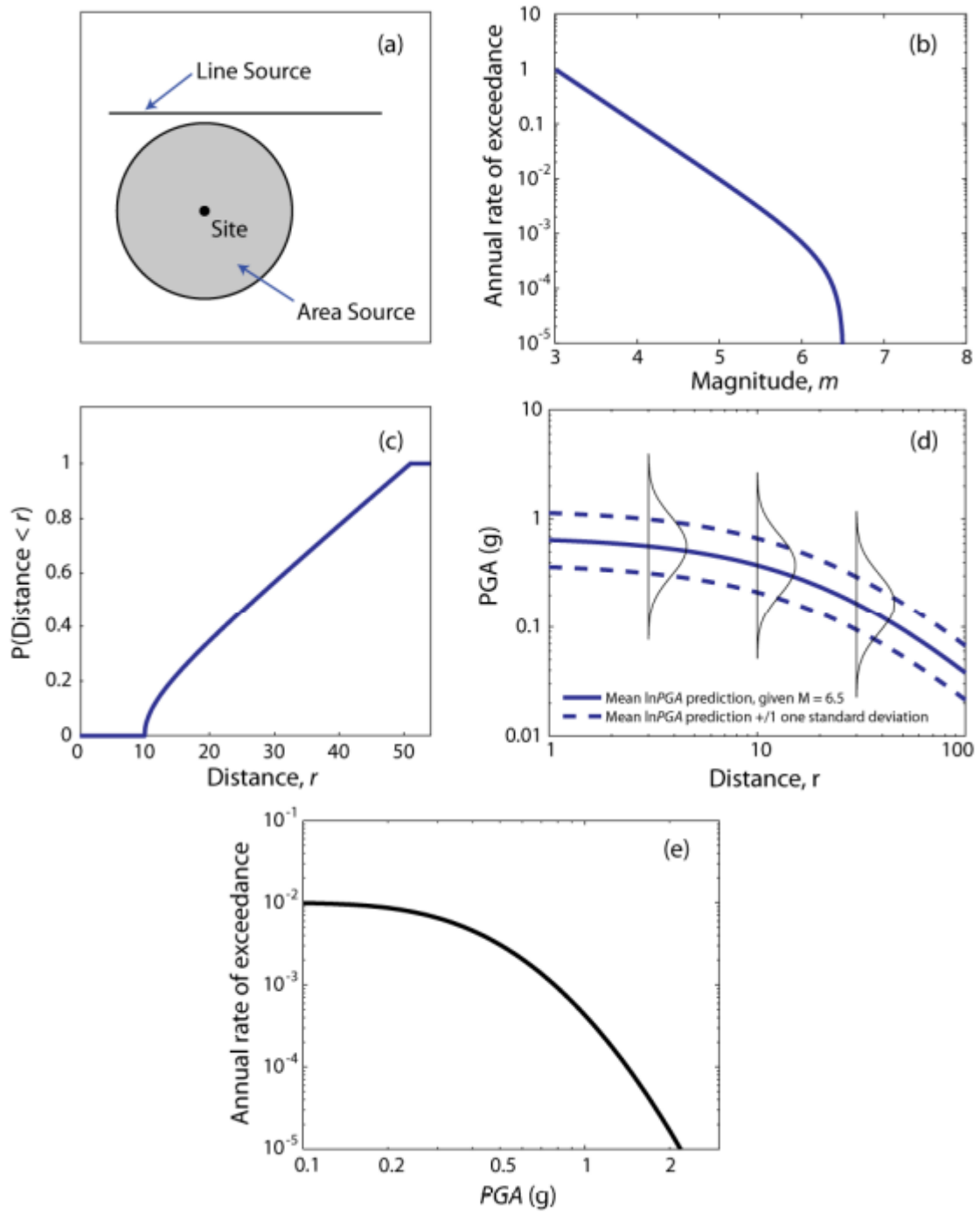


Figure 15 : Schematic illustration of the basic five steps in PSHA

3.2 Identification of seismic sources

Here, we are interested in all earthquake sources capable of causing harmful ground movements at a site, in contrast to the deterministic thinking discussed above, which concentrated primarily on the greatest potential earthquake event. Faults, which are generally flat surfaces and may be located using a variety of techniques, including observations of the sites of previous earthquakes and geological data, could be one of these sources. If specific faults cannot be located (as in the less seismically active areas in the east of the United States), then earthquake sources can be represented by general geographic areas where earthquakes may occur anywhere. The distribution of earthquake magnitudes and source-to-site distances may be determined once all potential sources have been determined.

3.3 Quantifying the seismicity Rate of Sources (The development of Magnitude-Recurrence Relationships for all sources).

Tectonic faults may cause earthquakes of different sizes (i.e., magnitudes). In their initial examination of earthquake magnitude measurements, Gutenberg and Richter (1944) found that there is a basic pattern to the distribution of earthquake sizes in a region, given as follows

$$\text{Log } \lambda_m = a - bm \quad (1.1)$$

Where a and b are constants and λ_m is the frequency of earthquakes with magnitudes larger than m . The term "Gutenberg-Richter recurrence law" refers to this equation.

The Gutenberg-Richter recurrence rule from the previous equation is shown alongside typical measurements from a fault or area in Figure 16.

Using statistical analysis of historical records and additional constraining information from various forms of geological evidence, the a and b constants from the aforementioned equation are calculated. The a value represents the total frequency of earthquakes in a given area, while the b value represents the proportion of earthquakes of small and big magnitudes (average b values are about equal to 1).

The magnitudes of earthquakes greater than a certain minimum magnitude m_{\min} can also be calculated using Equation 1.1 to produce a cumulative distribution function (CDF) (this

conditioning is used because earthquakes smaller than m_{\min} will be disregarded in subsequent calculations due to their lack of engineering importance).

$$\begin{aligned}
F_M(m) &= P(M \leq m | M > m_{\min}) \\
&= \frac{\text{Rate of earthquakes with } m_{\min} < M \leq m}{\text{Rate of earthquakes with } m_{\min} < M} \\
&= \frac{\lambda_{m_{\min}} - \lambda_m}{\lambda_{m_{\min}}} \\
&= \frac{10^{a-bm_{\min}} - 10^{a-bm}}{10^{a-bm_{\min}}} \\
&= 1 - 10^{-b(m-m_{\min})}, \quad m > m_{\min}
\end{aligned} \tag{1.2}$$

Where $F_m(m)$ denotes the cumulative distribution function for M . One can compute the probability density function (PDF) for M by taking the derivative of the CDF.

$$\begin{aligned}
f_M(m) &= \frac{d}{dm} F_M(m) \\
&= \frac{d}{dm} [1 - 10^{-b(m-m_{\min})}] \\
&= b \ln(10) 10^{-b(m-m_{\min})}, \quad m > m_{\min}
\end{aligned} \tag{1.3}$$

Where $f_m(m)$ denotes the probability density function for M .

We should be aware that the Gutenberg-Richter rule in equation 1.1, which in theory promises magnitudes with no upper bound but is unachievable due to physical limitations, is the basis for the PDF given in equation 1.3. Due to the restricted size of the source faults, there is often a cap on the maximum earthquake magnitude that may occur in a given location (earthquake magnitude is related to the area of the seismic rupture). If a maximum magnitude can be determined, then equation 1.2 becomes

$$F_M(m) = \frac{1 - 10^{-b(m-m_{\min})}}{1 - 10^{-b(m_{\max}-m_{\min})}}, \quad m_{\min} < m < m_{\max} \tag{1.4}$$

And equation 1.3 becomes

$$f_M(m) = \frac{b \ln(10) 10^{-b(m-m_{\min})}}{1 - 10^{-b(m_{\max}-m_{\min})}}, \quad m_{\min} < m < m_{\max} \quad (1.5)$$

Where m_{\max} is the largest earthquake a certain source is capable of producing. A bounded Gutenberg-Richter recurrence rule is what is used to describe this small size distribution. Figure 1.6 displays illustrative observations of earthquake magnitudes together with the fit Gutenberg-Richter and bounded Gutenberg-Richter recurrence laws.

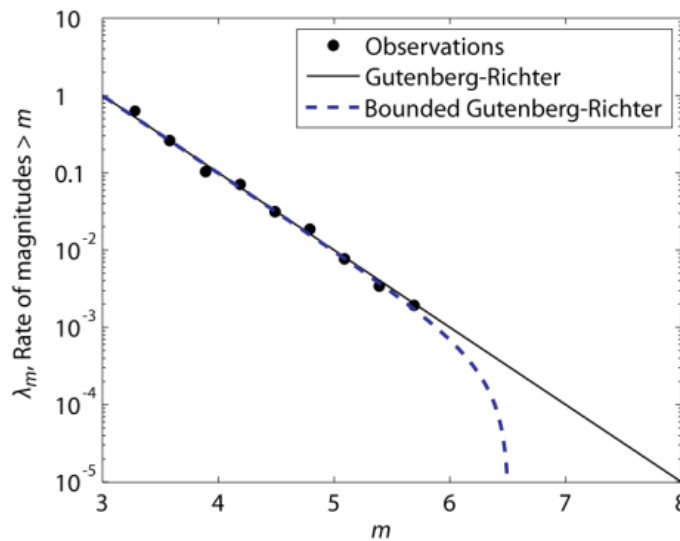


Figure 16: Typical distribution of observed earthquake magnitude

3.4 The selection of attenuation Model (or Ground Motion Prediction Equations, GMPEs)

It is also required to simulate the distribution of earthquake distances from the site of interest in order to anticipate ground shaking at a particular location. Every place along the fault is thought to have an identical chance of experiencing an earthquake for a particular earthquake source. The distribution of source-to-site distances can typically be determined using simply the source's geometry since locations are equally distributed.

Despite the fact that "distance" appears to have a clear definition, PSHA frequently uses a number of different definitions. The closest point on the rupture surface, the epicentre or hypocentre, or the surface projection of the rupture's closest point can all be used as measures of distance. It should be noted that certain definitions of distance take the rupture's depth into account, whilst others merely take its distance from the surface projection into consideration.

Furthermore, it should be noted that definitions based on the epicentre and hypocentre need only take the location of the rupture's beginning into account; other definitions, however, must explicitly take into account the fact that ruptures frequently occur over a plane rather than at a single point in space.

3.4.1 Attenuation Relationships

Ground motion attenuation is often represented by the form;

$$\text{Log } Y = C_1 + C_2.M + C_3.\text{Log}R + C_4.R + C_5.F + C_6.S + \mathcal{E}$$

Where

Y is the ground motion parameters of interest (i.e. PGA, PGV, SA, SD)

M is earthquake magnitude

R is source to site distance

F is the faulting mechanism of the earthquake

S is a description of the local site conditions

\mathcal{E} is a random error term that characterises the variability in ground motion. It has a mean of zero and a standard deviation of S (a Gaussian probability distribution).

Coefficients c_1 , c_2 , c_3 , c_4 , c_5 , and c_6 are often found by performing statistical regression analysis to fit the equation to the real ground motion data.

The term $C_3.\text{Log}R$ shows how the seismic wave front's geometric attenuation as it moves away from the earthquake's source.

The term $C_4.R$ depicts the elastic attenuation brought on by the damping and dispersion of the materials caused by the seismic waves' propagation through the crust.

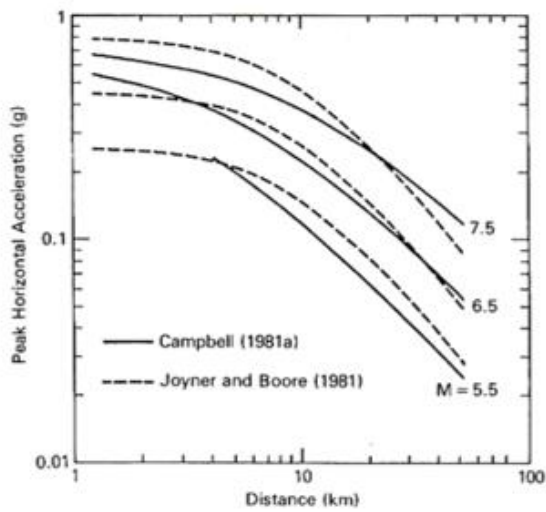
Some of the examples of the coefficients of an attenuation are given below

Coefficients of an attenuation relationship

TABLE 5.11 Coefficients for Sadigh et al. Rock Attenuation Relation: Horizontal Component

T_n (s)	c_1	c_2	c_3	c_4	c_5	c_6	c_7	c_8	c_9	c_{10}	c_{11}	c_{12}	c_{13}	c_{14}
$M_w \leq 6.5$														
PGA	0.182	-0.624	1.0	0	-2.100	0	3.6564	0.250	0	1.39	0.14	0.38	0	7.21
0.05	0.182	-0.090	1.0	0.006	-2.128	-0.082	3.6564	0.250	0	1.39	0.14	0.38	0	7.21
0.07	0.182	0.110	1.0	0.006	-2.128	-0.082	3.6564	0.250	0	1.40	0.14	0.39	0	7.21
0.09	0.182	0.212	1.0	0.006	-2.140	-0.052	3.6564	0.250	0	1.40	0.14	0.39	0	7.21
0.10	0.182	0.275	1.0	0.006	-2.148	-0.041	3.6564	0.250	0	1.41	0.14	0.40	0	7.21
0.12	0.182	0.348	1.0	0.005	-2.162	-0.014	3.6564	0.250	0	1.41	0.14	0.40	0	7.21
0.14	0.182	0.307	1.0	0.004	-2.144	0	3.6564	0.250	0	1.42	0.14	0.41	0	7.21
0.15	0.182	0.285	1.0	0.002	-2.130	0	3.6564	0.250	0	1.42	0.14	0.41	0	7.21
0.17	0.182	0.239	1.0	0	-2.110	0	3.6564	0.250	0	1.42	0.14	0.41	0	7.21
0.20	0.182	0.153	1.0	-0.004	-2.080	0	3.6564	0.250	0	1.43	0.14	0.42	0	7.21
0.24	0.182	0.060	1.0	-0.011	-2.053	0	3.6564	0.250	0	1.44	0.14	0.43	0	7.21
0.30	0.182	-0.057	1.0	-0.017	-2.028	0	3.6564	0.250	0	1.45	0.14	0.44	0	7.21
0.40	0.182	-0.298	1.0	-0.028	-1.990	0	3.6564	0.250	0	1.48	0.14	0.47	0	7.21
0.50	0.182	-0.588	1.0	-0.040	-1.945	0	3.6564	0.250	0	1.50	0.14	0.49	0	7.21
0.75	0.182	-1.208	1.0	-0.050	-1.865	0	3.6564	0.250	0	1.52	0.14	0.51	0	7.21
1.0	0.182	-1.705	1.0	-0.055	-1.800	0	3.6564	0.250	0	1.53	0.14	0.52	0	7.21
1.5	0.182	-2.407	1.0	-0.065	-1.725	0	3.6564	0.250	0	1.53	0.14	0.52	0	7.21
2.0	0.182	-2.945	1.0	-0.070	-1.670	0	3.6564	0.250	0	1.53	0.14	0.52	0	7.21
3.0	0.182	-3.700	1.0	-0.080	-1.610	0	3.6564	0.250	0	1.53	0.14	0.52	0	7.21
4.0	0.182	-4.230	1.0	-0.100	-1.570	0	3.6564	0.250	0	1.53	0.14	0.52	0	7.21
5.0	0.182	-4.714	1.0	-0.100	-1.540	0	3.6564	0.250	0	1.53	0.14	0.52	0	7.21
7.5	0.182	-5.530	1.0	-0.110	-1.510	0	3.6564	0.250	0	1.53	0.14	0.52	0	7.21

activate window
Go to Settings to activate



Median (50th percentile) estimates for peak horizontal acceleration from Campbell (1981a) and Joyner and Boore (1981). Joyner and Boore (1981) estimates of the maximum horizontal component have been reduced by 12% so that they may be compared with the (Campbell 1981a) estimates of the mean horizontal component (after Campbell 1981a).

Figure 17: Campbell and Joyner & Boore Ground Motion Prediction Equations

In Figure 17, two examples are given Campbell (1981a) and Joyner & Boore (1981). These are the two ground motion prediction equations and Campbell is represented with a solid line for different magnitudes. Joyner and Boore is represented with dotted line for different magnitude as well. So the graph implies that as the distance increases the peak ground acceleration (g) decreases.

3.4.2 Random Error of Attenuation Model.

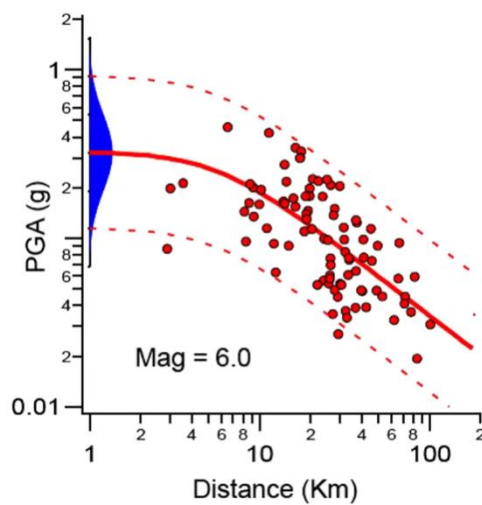


Figure 18PGA graph

The graph in the above figure shows the random error of attenuation Model. The dots represents the actual data and the red line is the mean value of the ground motion prediction equation. The data will be above and below the mean line which will having Gaussian Probability distribution. The errors is represented through the epsilon term in the GMPE. So the Epsilon value is basically the random error in the GMPE.

3.4.3 Source to site Distance

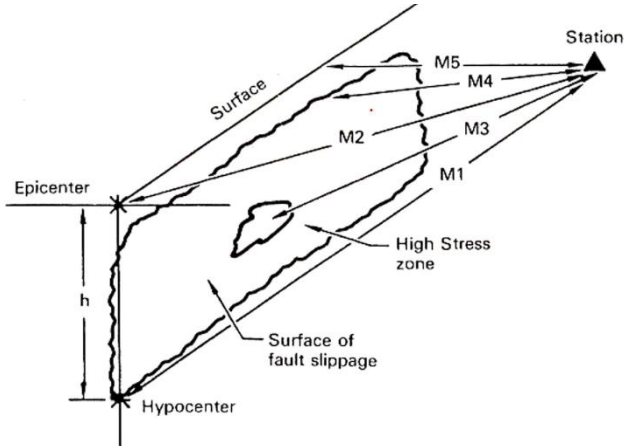


FIGURE 7.3 Schematic illustration of methods of distance measurement used in the determination of the distance value to be associated with a ground motion observation. M1 is the hypocentral distance (local depth is h), M2 is the epicentral distance. M3 is the distance to the center of high-energy release (or high localized stress drop), M4 is the closest distance to the slipped fault, in this case, the fault rupture does not extend to the surface, and M5 is the closest distance to the surface projection of the fault rupture (after Shakal and Bernreuter 1981).

Figure 19 Source to site distance

Similarly the source to site distance which is on the x axis of the GMPE. Here M1 to M5 represents the source to site distances but they all have different definitions. M1 here represents the hypocentre distance. Similar M2 is the epicentre distance. So these are the two different source to site definition but there can be others also. For example, M3 is the closest distance to the centre of the high energy release. Although the rupture originally originated from Hypocentre the high energy release is in the middle. From that point to the station represents the M3. M4 is the closest distance from slip/rupture to the station. And if taken the projection from that actual rupture/slip on the surface, from that surface to the station will be M5. So here we can see different source to site definition. So it's necessary to check while using GMPE, what definition of source to site distance that GMPE actually used.

3.4.4 Faulting Mechanism

Table 2 Faulting Mechanism

Faulting Mechanism Categories and Related Rake Angles for Selected Attenuation Relations

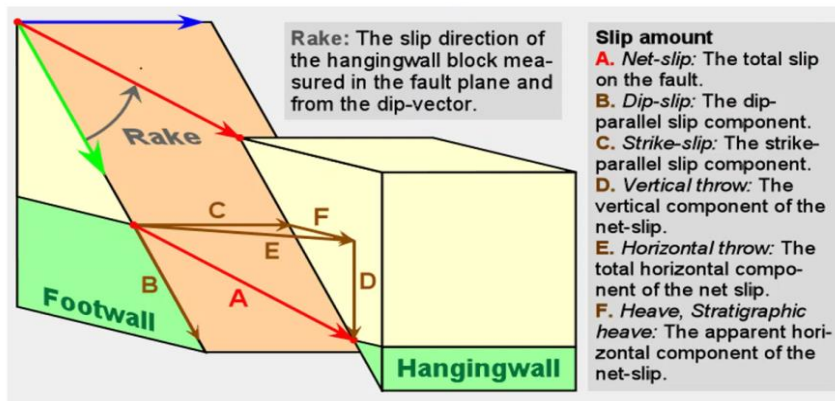
Attenuation Relation	Category	F	Rake Angle (λ)
Abrahamson and Silva [1997]	Strike slip	0	0–30°, 150–210°, 330–360°
	Normal	0	210–330°
	Reverse-oblique	0.5	30–60°, 120–150°
	Reverse	1.0	60° to 120°
Boore et al. [1997]	Strike slip	—	0–30°, 150–210°, 330–360°
	Normal	—	210–330°
	Unknown	—	Unknown or random
	Reverse	—	30–150°
Campbell and Bozorgnia [in press]	Strike slip	0	0–22.5°, 177.5–202.5°, 337.5–360°
	Normal	0	202.5–337.5°
	Reverse ($F_{RV}=1$)	1.0	22.5–157.5° ($\delta > 45^\circ$)
	Thrust ($F_{TH}=1$)	1.0	22.5–157.5° ($\delta \leq 45^\circ$)
Sadigh et al. [1993, 1997]	Strike slip	0	0–45°, 135–225°, 315–360°
	Normal	0	225–315°
	Reverse	1.0	45–135°
Spudich et al. [1999]	Strike slip	—	0–45°, 135–225°, 315–360°
	Normal	—	225–315°

Note: Unless otherwise indicated, an unknown or random faulting mechanism is given by $F = 0.5$, $F_{RV} = 0.25$, and $F_{TH} = 0.25$.

So in GMPEs, we know that magnitude is one of the basic inputs. The magnitude should be kept fixed and then come up with the PGA value for a given source to site distances. So R, M are known inputs but there can be other input parameters for example one of them is the faulting Mechanism which is represented by Fin different GMPEs.

For different types or Categories, there will be different F factors. So the effect of different Faulting mechanism is considered in GMPEs using this factor. In the above table we can see that different attenuation relationship is compared here. The Rake angle is defined and these will be different for different types of Faults.

3.4.5 Slip Terminology



Source: <https://www.naturalfractions.com/>

Figure 20 Slip Terminology

When there is a slip, there can be different kinds of slip terminology. For example the A distance is the net slip (total slip of the faults). The faults can have lateral slip as well as dip slip. B is the actual dip slip. C is strike slip and D is the Vertical throw (it is the amount by which the one part of the block of the earth has moved down compared to other part.) E is horizontal throw and F is the apparent horizontal component of the net slip.

So the summary, is that the actual Faulting mechanism is also accounted in the GMPEs using F factor and i.e. for different types of faults will have different F factors.

3.4.6 Local site conditions

Table 3 Building Code Site classes

Definition of Building-Code Site Classes			
Site Class	Soil Profile Name	30-m Velocity, V_{530} (m/sec)	
		Range	Average
A	Hard rock	>1,500	1890
B	Rock	760–1500	1130
BC	BC boundary	555–1000	760
C	Very dense soil and soft rock	360–760	560
CD	CD boundary	270–555	360
D	Stiff soil	180–360	270
DE	DE boundary	90–270	180
E	Soft soil	<180	150

Source: Adapted from Wills, C.J. et al. 2000. "A Site-Conditions Map for California Based on Geology and Shear-Wave Velocity," *Bull. Seismol. Soc. Am.*, 90, S187–S208. With permission.

One of the important parameters of GMPEs is the Local Site Conditions. We know that different building code basically classify the sites based on the quality of soil or types of soil based on the site classes. The shear wave velocity of the first 30m of the soil layer which is also called V_{s30} is an important parameter which basically tells about the stiffness of the soil. So the hard rocks will have high V_{s30} value compared to soft soil.

4. Ground motion intensity

Our concentration is on ground motion studies rather than earthquakes, however we have already computed the distribution of potential earthquake magnitudes and epicentres. The natural next step is a ground motion prediction model. According to a number of predictor criteria, such as the size, position, faulting process, site conditions at the surface, the potential for directivity effects, etc., these models predict the probability distribution of ground motion intensity. Given the large number of predictor variables, we usually say that the model predicts ground motion intensity given "magnitude, distance, etc.

5. The Development of Hazard Curves for the sites.

Basic techniques for figuring out a site's seismic hazard potential include doing a probabilistic seismic hazard analysis and making seismic hazard curves. A seismic hazard curve is produced by incorporating data from many sources and shows the correlation between a seismic intensity measure, such as peak ground acceleration (PGA), and its annual likelihood of surpassing it. These details include the identification of the earthquake sources nearby the site, the arrival rate of the earthquake, and the magnitude of the earthquake, along with the probability density function of the earthquake magnitude and the seismic intensity parameter, which is typically expressed as peak ground acceleration (PGA) at the site for likely earthquakes occurring at the sources.

So in the last step, we will use or combine the information from step 2 and step 3 to construct the Hazard Curve of the site. This curve will have, the probability of exceedances or the cumulative annual frequency on Y axis and ground motion parameters on x axis.

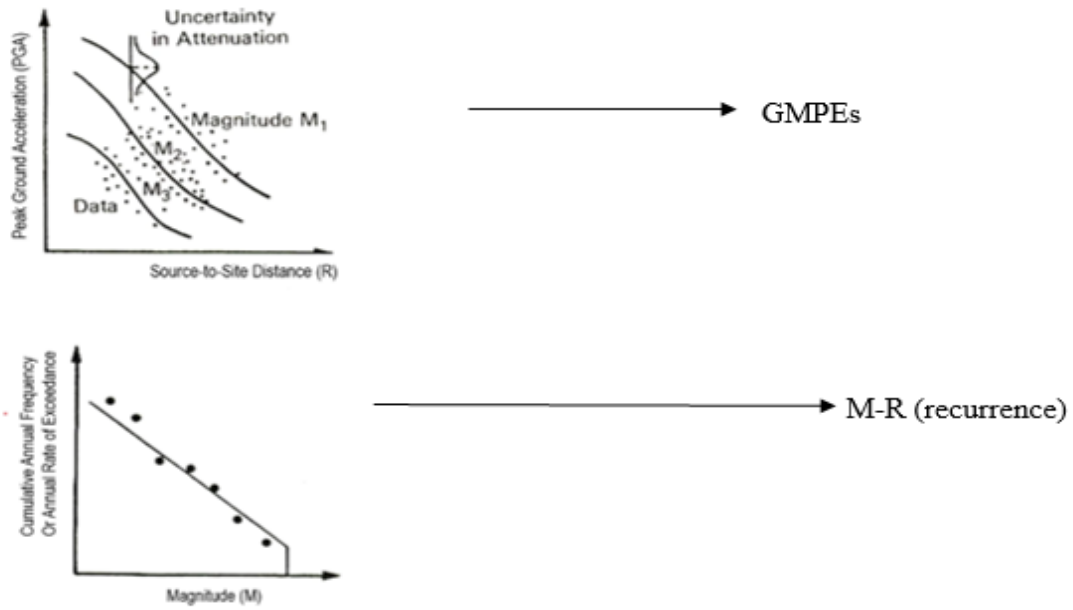


Figure 21 GMPE and M-R

After selecting GMPEs and M-R for each of the seismic source, now to construct the Hazard Curve for the site. We need to select a PGA value let's say 0.1g and we also know the source to site distance. Drawing an interpolation of PGA and source to site distance(R) will result in the corresponding Magnitude value. Let's denote the magnitude value as M.

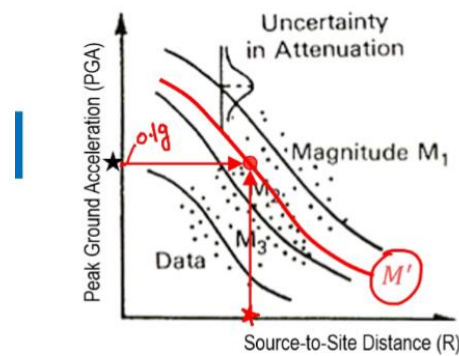


Figure 22 PGA to Distance Graph

Now using that M' value, we come to our magnitude recurrence relation graph.

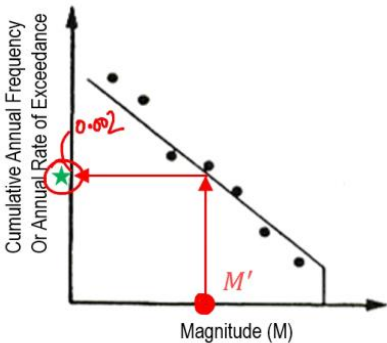


Figure 23 Probability of exceedence

In the graph the corresponding M' will result in a value say 0.002 which will be Cumulative Annual frequency or annual rate of occurrence. As the annual rate of occurrence can also be expressed as the probability of exceedence, constructing a new curve which has Y axis as Annual Rate of Exceedance or Probability of exceedance and X axis as PGA Value.

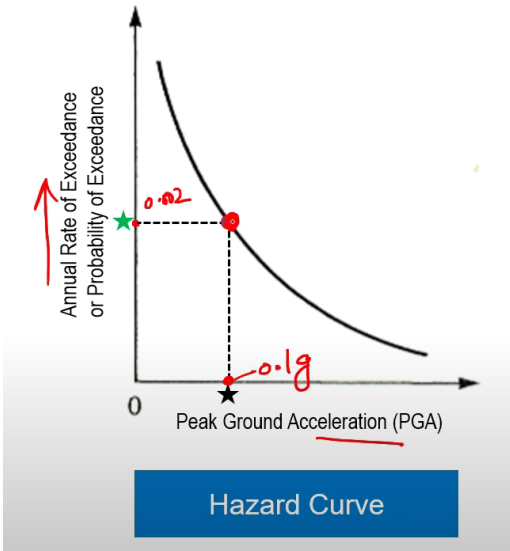


Figure 24 Hazard Curve

Now corresponding to 0.1g and 0.002 we get a point on the curve. Similarly repeating the process by selecting a different PGA values will result in multiple points on the curve. Eventually the curve represents the level of hazard at the sites according to the different definition of hazards. For example we can define a hazard definition of earthquake as 10 %

Probability Exceedance (PE) in 50 yrs. So we can convert the 10% PE into the annual rate of exceedance. This is how we draw the Hazard Curve.

6. Site amplification analysis

The final stage of the seismic hazard assessment procedure is site amplification. As vertically transmitted shear waves go from the ground to the surface, it is well known that the ground motion substantially changes, especially if there are significant variations in the shear wave velocity across the layers of the soil model. The purpose of the amplification analysis is to create the ground motion response spectra (GMRS) (USNRC, 2007). A foundation input response spectrum (FIRS) refers to extra ground motion application locations that may be required and is a fictitious diagram showing the position of the GMRS and FIRS. The subsurface conditions must be stated in detail since the soil column's shear wave velocity is a crucial input for the amplification analysis. Therefore, a comprehensive geotechnical and geophysical investigation campaign is required.

7. Probabilistic Seismic Risk Assessment

A technique called probabilistic seismic risk analysis examines the potential of severe ground motion intensities that might destroy infrastructure and structures and disrupt social and economic activity. Initially, back in the days PSRA was used in nuclear power plants to assess any kind of endangerments like the risk of lethal radiations. Now it has been adopted by various fields to assess any probabilistic risk concerned with it.

The earthquake early warning (EEW) system, which gives individuals critical time to seek safety before the arrival of stronger seismic waves, uses probabilistic seismic risk assessment. For engineering design, it often uses probabilistic seismic hazard analysis. Based on the frequency of earthquakes and ground motion prediction equations (GMPEs), it calculates the likelihood of surpassing the ground motion level during a certain time period.

CHAPTER 5

DATA COLLECTION AND ANALYSIS

1. SITE LOCATION

Site code: IBRH13 Site name: TAKAHAGI, IBARAKIKEN Prefecture.

The site of our project is at a place called TAKAHAGI, IBARAKIKEN Prefecture of Japan. It is located at latitude of 36.7955 and Longitude at 140.5750. The altitude of the site is 505m.

Soil condition Data are collected as below:

Table 4 Soil Condition Data for TAKAHAGI

No	Thickness(m)	Depth (m)	Vp (m/s)	Vs (m/s)
1	1.00	1.00	250.00	170.00
2	15.00	16.00	460.00	280.00
3	8.00	24.00	2050.00	400.00
4	10.00	34.00	2050.00	600.00
5	10.00	44.00	3200.00	1050.00
6	32.00	76.00	4900.00	2600.00
7			4900.00	3000.00

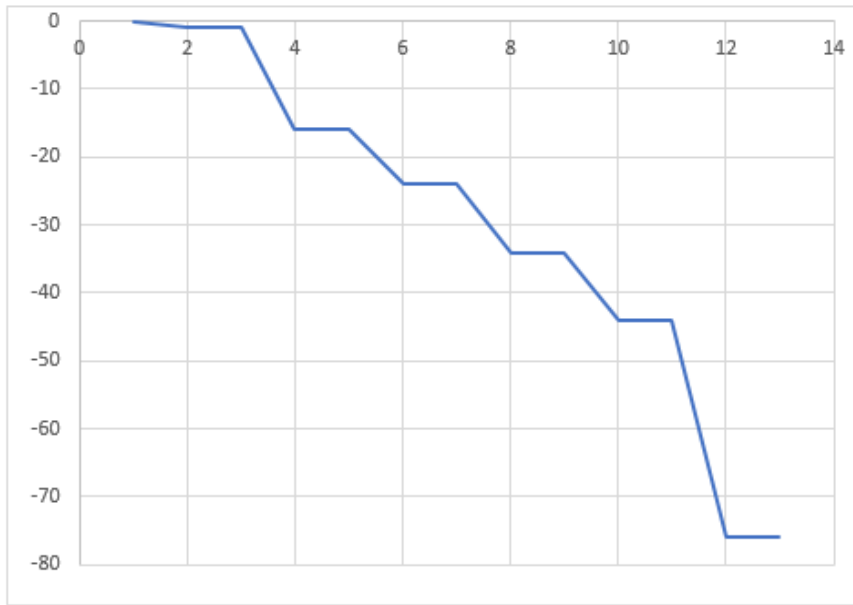


Figure 25 Soil Profile of Takahagi

Soil Profile Analysis is carried out as shown in Figure 25.

The Peak Acceleration Contour Map of Japan is as shown below:

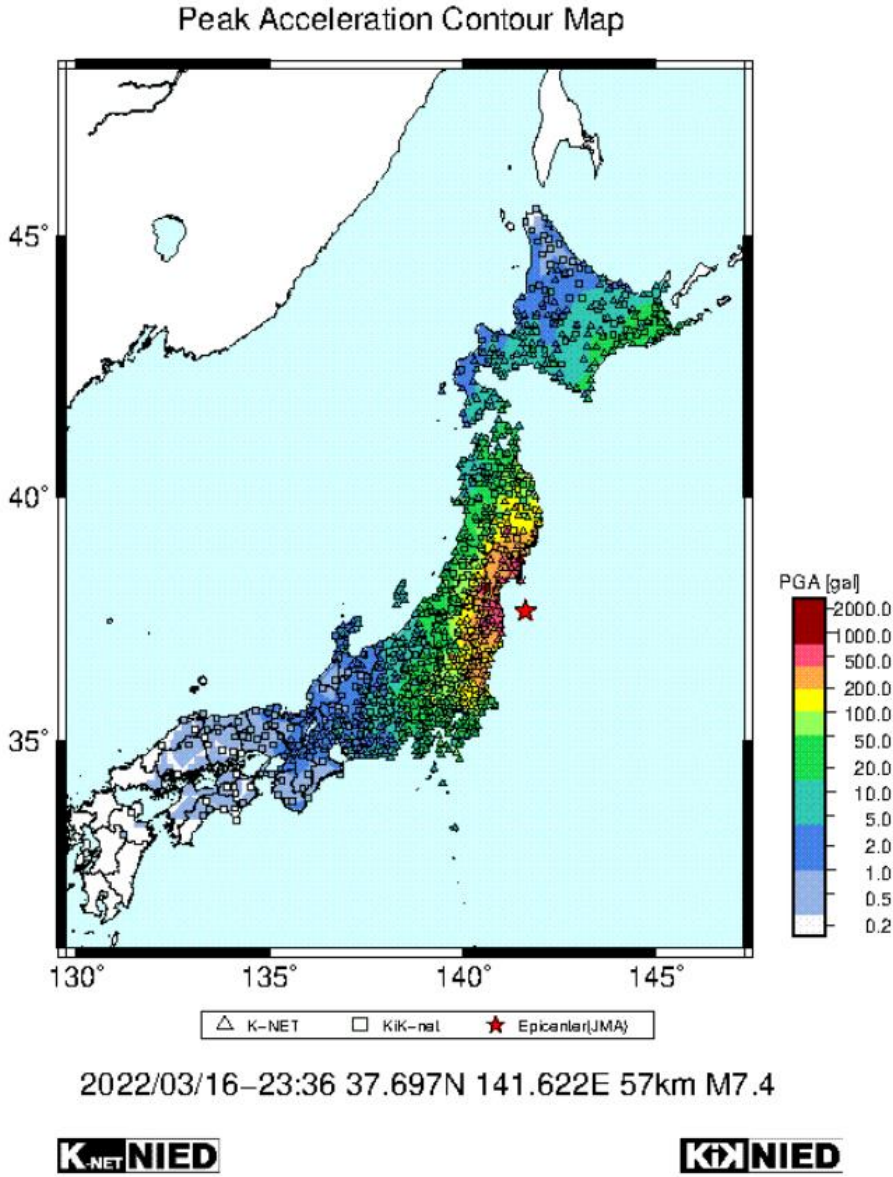


Figure 26 Peak Acceleration Contour Map of Japan

1. Data Collection

Strong Motion Data are collected from Kiknet Website as below:

GM #	Station	Station Lat.	Station Lon.	Record Date	Record Time	EQ Lat [from Fnet catalog]	EQ Lon [from Fnet catalog]	Mw [from Fnet catalog]	Strike1 [from Fnet catalog]	Dip1 [from Fnet catalog]	Rake1 [from Fnet catalog]	Strike2 [from Fnet catalog]	Dip2 [from Fnet catalog]	Rake2 [from Fnet catalog]	Focal Mech [Using Eqs in Garcia et al. 2011]	EQ category (Based on Allen et al)	R震源距 [km]	Azimuth (Degree)	R震源深 [km]	V30 (m/sec)	
1	17972	IBRH13	36.7924	140.578	10/17/04	2:19	36.272	141.406	5.3	28	72	89	213	18	95	RS	Shallow active crustal GMPE	93.8861	127.815	95.9926916	335.368718
2	17976	IBRH13	36.7924	140.578	10/27/04	10:41	37.289	139.037	5.8	218	60	100	18	32	73	RS	Shallow active crustal GMPE	147.464	292.429	147.873936	335.368718
3	17990	IBRH13	36.7924	140.578	5/15/05	15:55	36.629	139.485	4.3	76	84	165	168	75	7	SS	Shallow active crustal GMPE	99.0896	259.788	99.4102133	335.368718
4	18081	IBRH13	36.7924	140.578	5/5/08	9:27	36.279	141.877	4.9	14	72	81	220	20	115	RS	Shallow active crustal GMPE	129.241	115.806	130.779311	335.368718
5	66128	IBRH13	36.7924	140.578	2/28/04	18:34	36.691	142.155	4.8	13	76	85	214	14	111	RS	Shallow active crustal GMPE	140.814	94.1313	142.227623	335.368718
6	84153	IBRH13	36.7955	140.575	4/30/10	19:34	36.302	139.147	3.8	331	60	39	219	57	143	ALL	Shallow active crustal GMPE	138.79	247.129	140.22832	335.368718
7	84600	IBRH13	36.7955	140.575	5/1/10	18:21	37.559	139.191	4.6	33	47	85	220	44	95	RS	Shallow active crustal GMPE	149.034	305.125	149.249015	335.368718
8	88126	IBRH13	36.7955	140.575	9/30/10	1:23	37.281	140.006	4.2	162	64	68	24	33	127	RS	Shallow active crustal GMPE	73.8476	317.077	74.2796983	335.368718
9	89204	IBRH13	36.7955	140.575	10/1/10	8:24	37.248	140.027	4.3	198	67	93	10	23	83	RS	Shallow active crustal GMPE	69.9025	316.097	70.0811056	335.368718
10	97773	IBRH13	36.7924	140.578	11/5/09	7:02	38.4	142.311	4.8	307	74	-105	171	22	-48	NM	Shallow active crustal GMPE	234.84	40.0697	235.256966	335.368718
11	97782	IBRH13	36.7955	140.575	3/12/11	3:59	36.982	138.598	6.2	29	56	70	242	38	117	RS	Shallow active crustal GMPE	176.984	277.462	177.054927	335.368718
12	97789	IBRH13	36.7955	140.575	3/14/11	10:02	36.458	141.125	5.7	227	72	-28	327	63	-160	ALL	Shallow active crustal GMPE	61.7436	127.198	62.2597001	335.368718
13	97800	IBRH13	36.7955	140.575	3/19/11	18:56	36.784	140.572	5.8	141	48	-94	327	42	-86	NM	Shallow active crustal GMPE	13.477	193.363	15.1784457	335.368718
14	97807	IBRH13	36.7955	140.575	3/23/11	7:12	37.085	140.788	5.7	191	64	-94	20	27	-82	NM	Shallow active crustal GMPE	37.2911	30.3879	37.6247994	335.368718
15	109732	IBRH13	36.7955	140.575	4/1/11	2:21	36.959	141.218	4.2	69	48	-67	217	47	-113	NM	Shallow active crustal GMPE	59.9829	72.1983	61.5950286	335.368718
16	109737	IBRH13	36.7955	140.575	4/2/11	19:22	36.82	140.569	4.1	179	67	-84	344	23	-104	NM	Shallow active crustal GMPE	2.81044	348.683	5.7357271	335.368718
17	109738	IBRH13	36.7955	140.575	4/2/11	23:38	37.097	140.834	4.6	246	62	-90	66	28	-90	NM	Shallow active crustal GMPE	40.5926	34.438	40.8993543	335.368718
18	109740	IBRH13	36.7955	140.575	4/3/11	10:54	37.094	140.809	3.9	246	62	-87	58	28	-96	NM	Shallow active crustal GMPE	39.1463	31.9169	39.4642774	335.368718
19	109751	IBRH13	36.7955	140.575	4/6/11	7:02	38.4	142.311	4.8	307	74	-105	171	22	-48	NM	Shallow active crustal GMPE	234.84	40.0697	235.256966	335.368718
20	109752	IBRH13	36.7955	140.575	4/6/11	21:56	36.735	140.603	4.7	163	59	-106	12	35	-66	NM	Shallow active crustal GMPE	7.18463	159.844	8.75322306	335.368718
21	109762	IBRH13	36.7955	140.575	4/9/11	18:01	36.941	140.607	4	241	86	-115	143	26	-9	ALL	Shallow active crustal GMPE	16.3789	9.89782	25.8508722	335.368718
22	109768	IBRH13	36.7955	140.575	4/11/11	11:00	36.701	140.656	3.6	163	65	-94	352	26	-81	NM	Shallow active crustal GMPE	12.7206	145.438	13.6801115	335.368718
23	109770	IBRH13	36.7955	140.575	4/11/11	17:16	36.946	140.673	6.6	132	50	-82	301	41	-99	NM	Shallow active crustal GMPE	18.1477	27.4617	19.4677608	335.368718
24	109774	IBRH13	36.7955	140.575	4/11/11	20:42	36.966	140.635	5.5	264	62	-92	89	28	-86	NM	Shallow active crustal GMPE	19.6822	15.7031	21.2459468	335.368718
25	109776	IBRH13	36.7955	140.575	4/12/11	0:21	36.841	140.514	4.5	49	48	-88	226	42	-93	NM	Shallow active crustal GMPE	7.45139	312.98	8.97346933	335.368718
26	109779	IBRH13	36.7955	140.575	4/12/11	0:58	37.062	140.653	4.7	180	54	-98	14	37	-79	NM	Shallow active crustal GMPE	30.4409	13.1842	30.8488131	335.368718

Figure 27 Strong Motion Data

The data applied in the analysis is of ground motions with two different amplitudes.

- PGA of GM1 = 0.1252 m/s²
- PGA of GM2 = 0.2448 m/s²

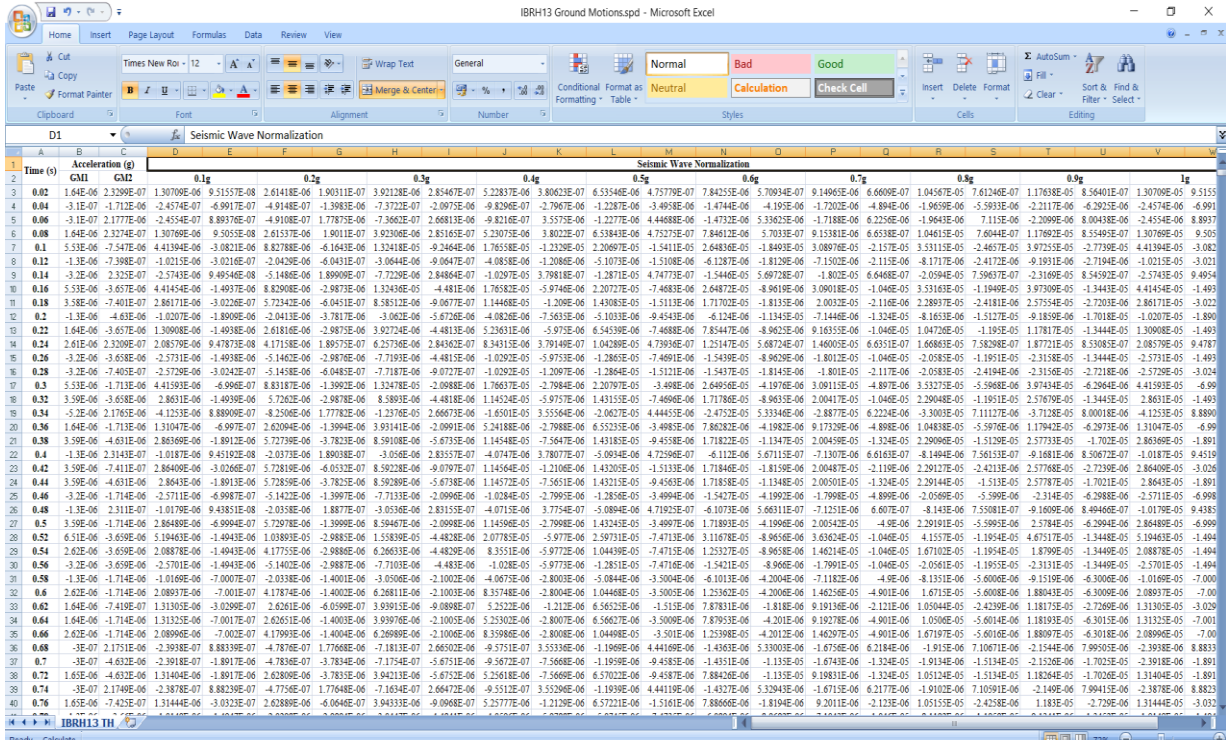


Figure 28 Spectral Data of GM with 2 amplitudes

2. Analysis of G+2 structural Model of a Hospital on Midas Gen 2021

1. Modeling a simple hospital

- Building : G+2
- Story height: 3m
- Dimension:
 - ✓ Beam:300x500mm
 - ✓ Column: 300x300mm
 - ✓ Plate thickness: 150mm
- Concrete Grade: M30

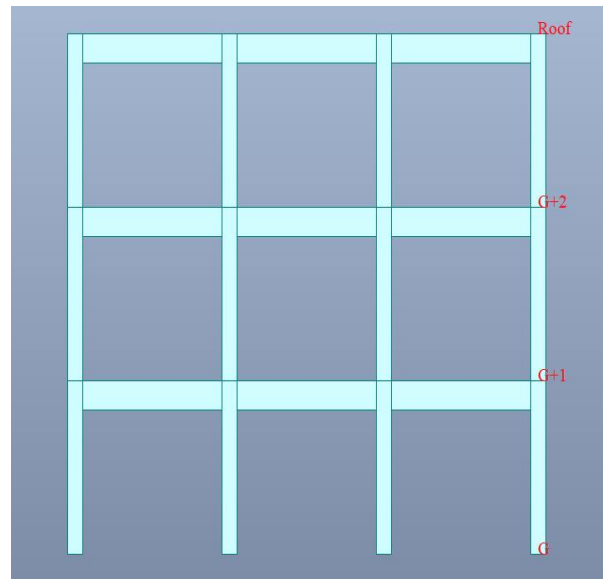


Figure 29 G+2 Hospital Model

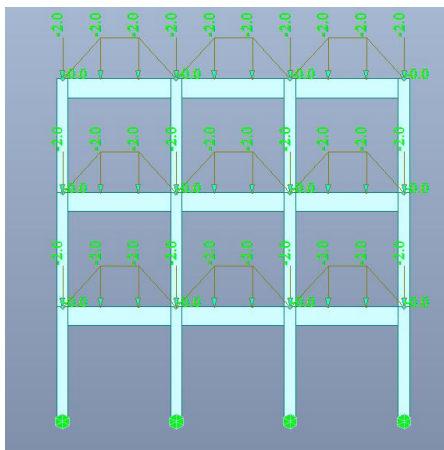


Figure 30 G+2 Hospital Model with load

- Loading cases
- Self-weight : -1(z- direction)
- Floor load
 - ✓ Dead load = -2kN/m^2
 - ✓ Live load = -4kN/m^2
- Roof load
 - ✓ Dead load = -2kN/m^2
 - ✓ Live load = -1.5kN/m^2

2. Performing Time History Analysis

The method of dynamic analysis being used to study the structural response is Time history analysis. Time history analysis is a type of structural analysis used to study the dynamic behaviour of structures subjected to time-varying loads or motions. It involves modelling the structure using mathematical equations and analyzing its response to the input load or motion over time. In time history analysis, the load or motion is specified as

a function of time, such as a sinusoidal, random, or seismic ground motion. The analysis involves solving the equations of motion of the structure using numerical methods, such as finite element analysis, to obtain the displacement, velocity, and acceleration responses of the structure when subjected to certain time varying loads.

The analysis helps engineers understand the dynamic response of structures to various loading conditions, including earthquake, wind, blast, and other transient events. It can be used to assess the structural integrity, identify potential failure modes, and design appropriate mitigation measures. Time history analysis is commonly used in the design of structures such as buildings, bridges, dams, and nuclear power plants. It is also used in the design of mechanical and aerospace systems, such as spacecraft, satellites, and aircraft

Here are the steps being followed to carry out time history analysis.

Upon adding all the static load cases, select the suitable type of Eigen value for the analysis.

- The natural frequencies and modes of vibration of a structure are examined using Eigen values. It chooses the vibration modalities and natural frequencies that the structure will vibrate at.
- The number of frequency is equal to the number of modes used to analyze the structure.

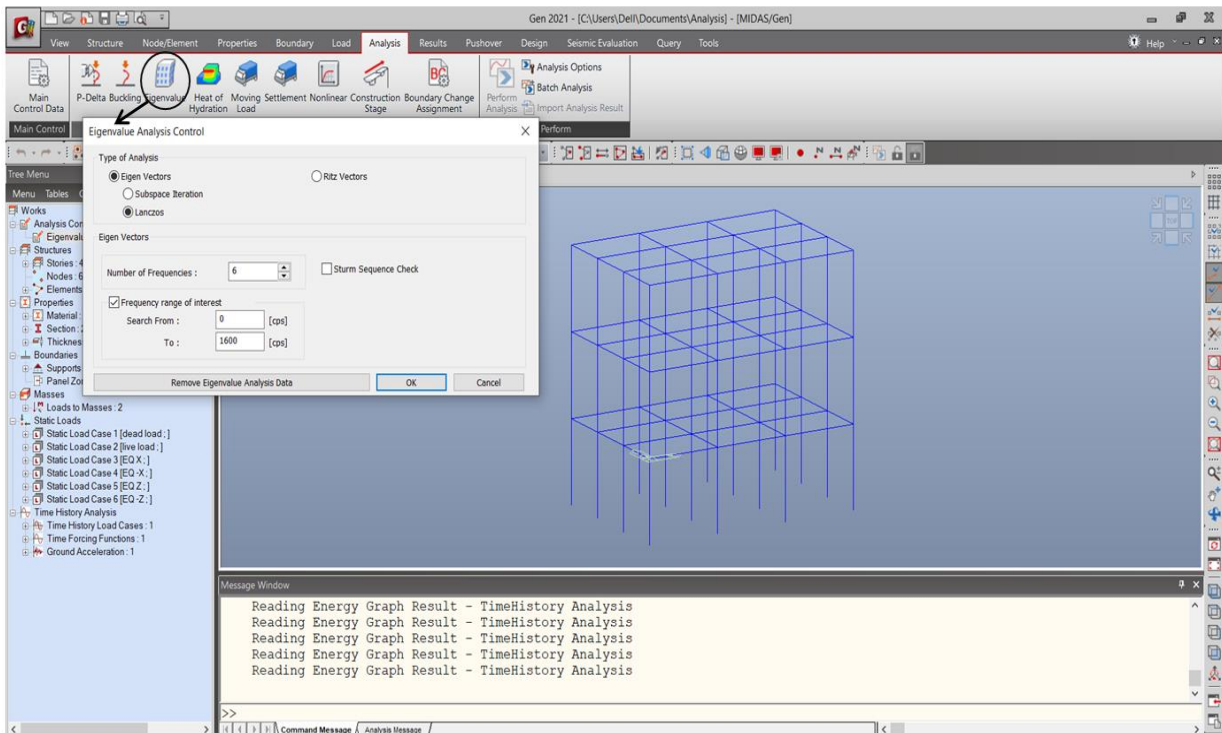


Figure 31 Applying Eigen Value

Next add the spectral data for the Time History Analysis. The analysis can generate both time history graph as well as response spectrum graph

- Similarly, the analysis was run twenty times for two different spectral acceleration data and the time history graphs are as follows.

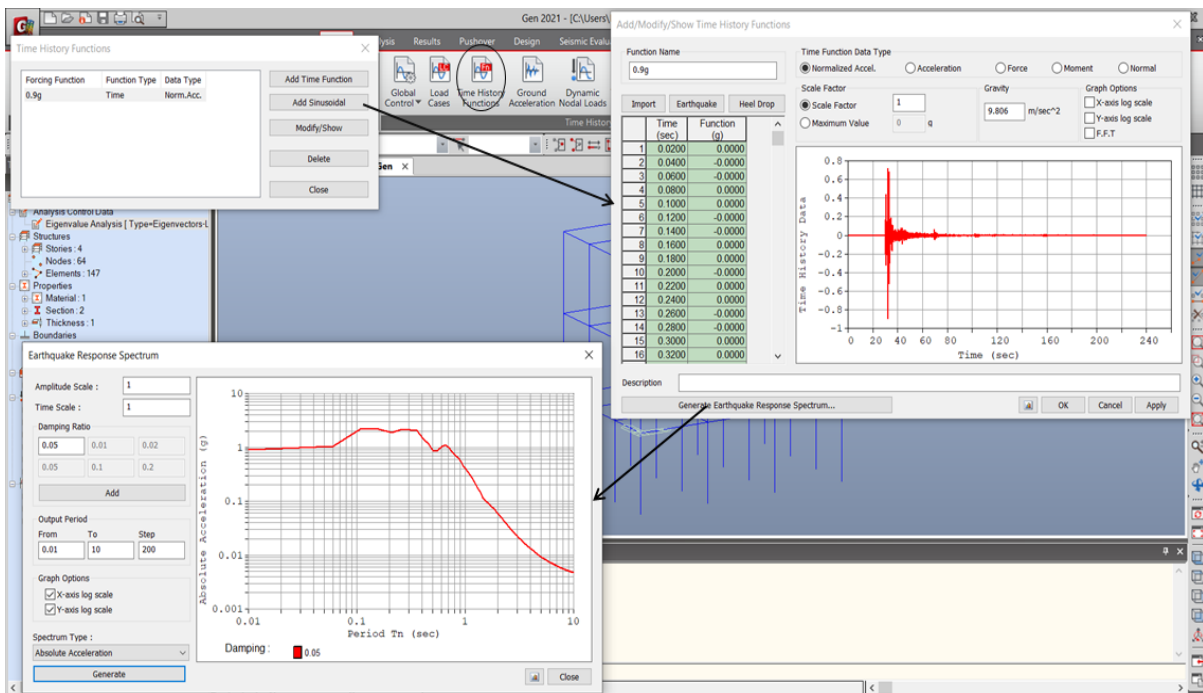


Figure 32 Spectral Data for the Time History Analysis

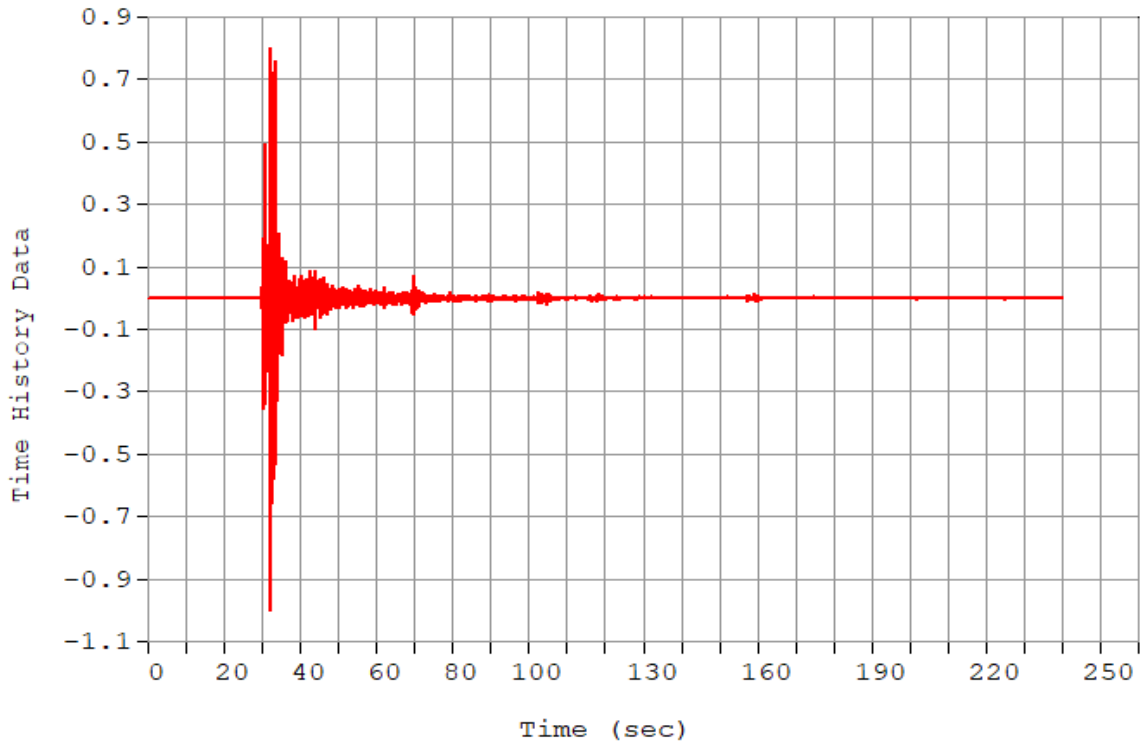


Figure 34 GM1 THA 1g

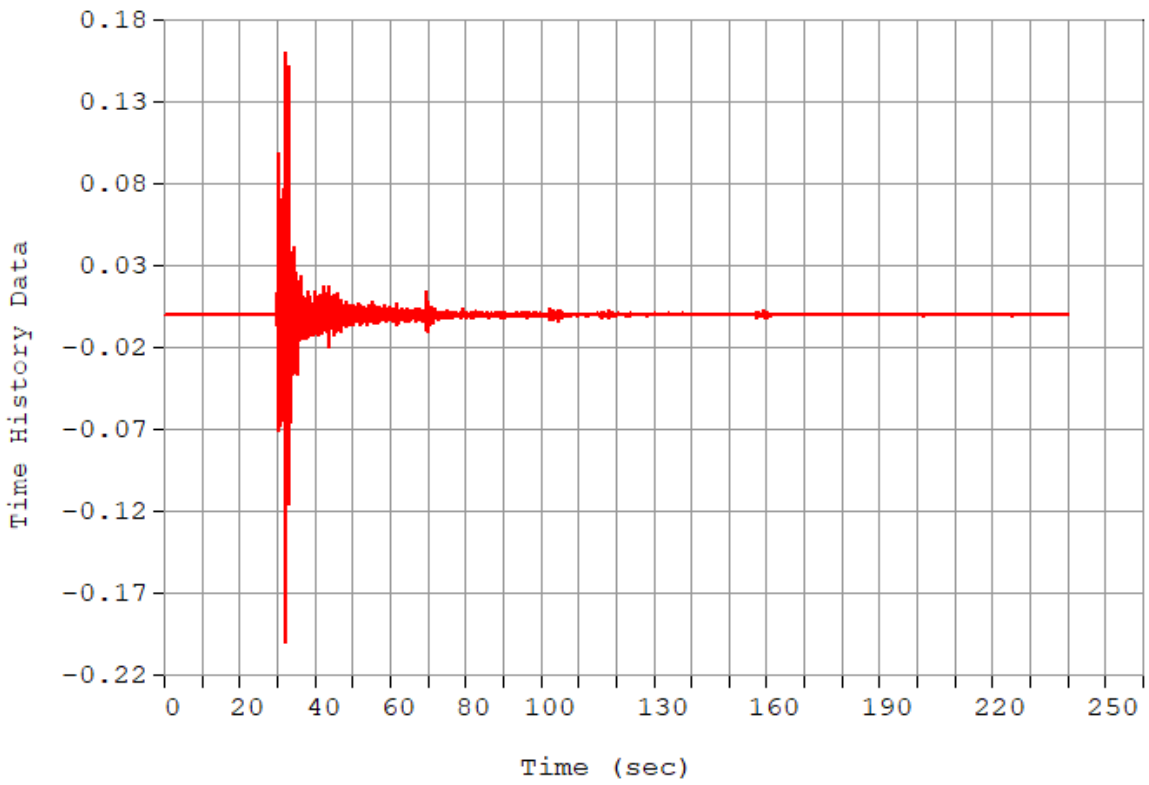


Figure 33 GM1 THA 0.2g

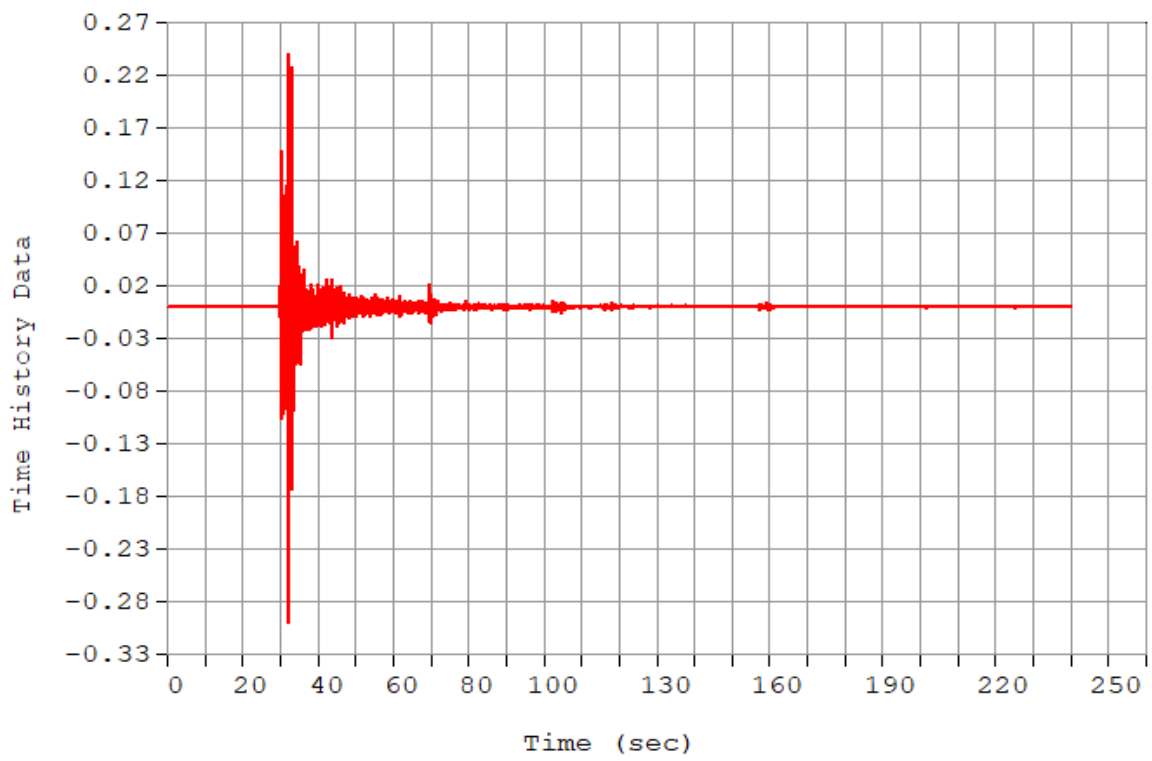


Figure 36 GM1 THA 0.3g

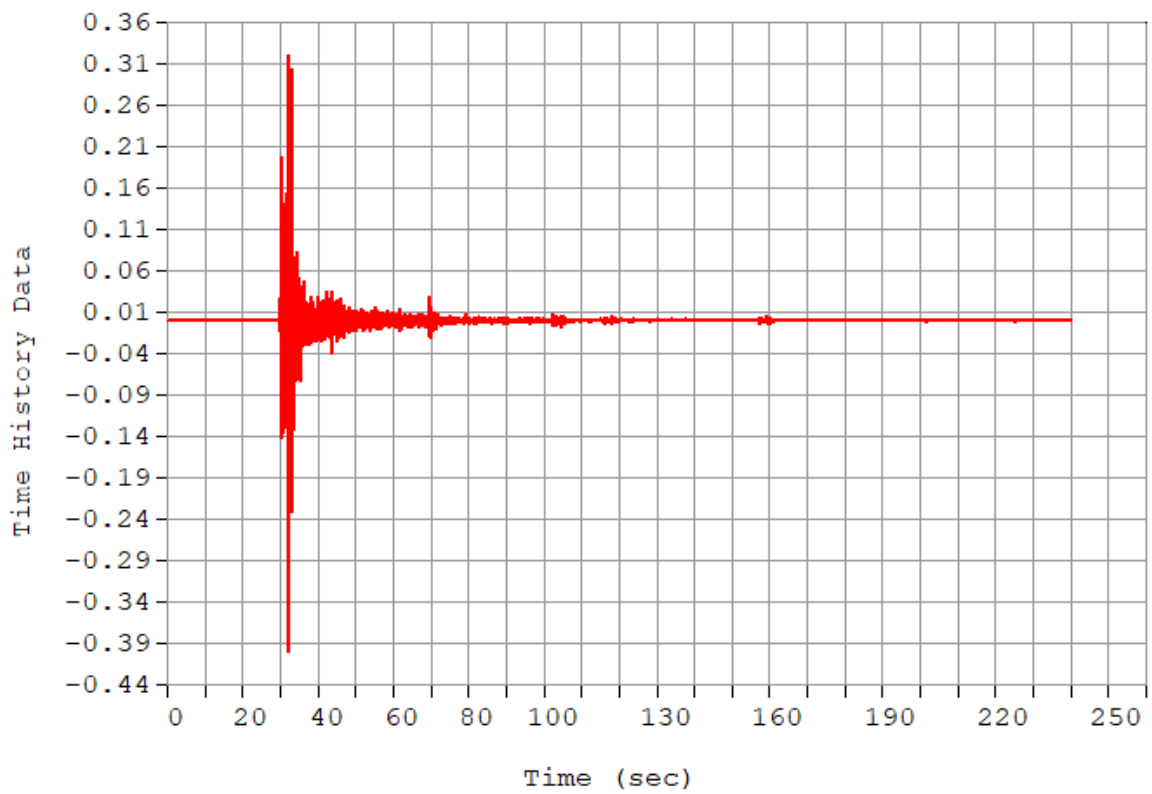


Figure 35 GM1THA 0.4g

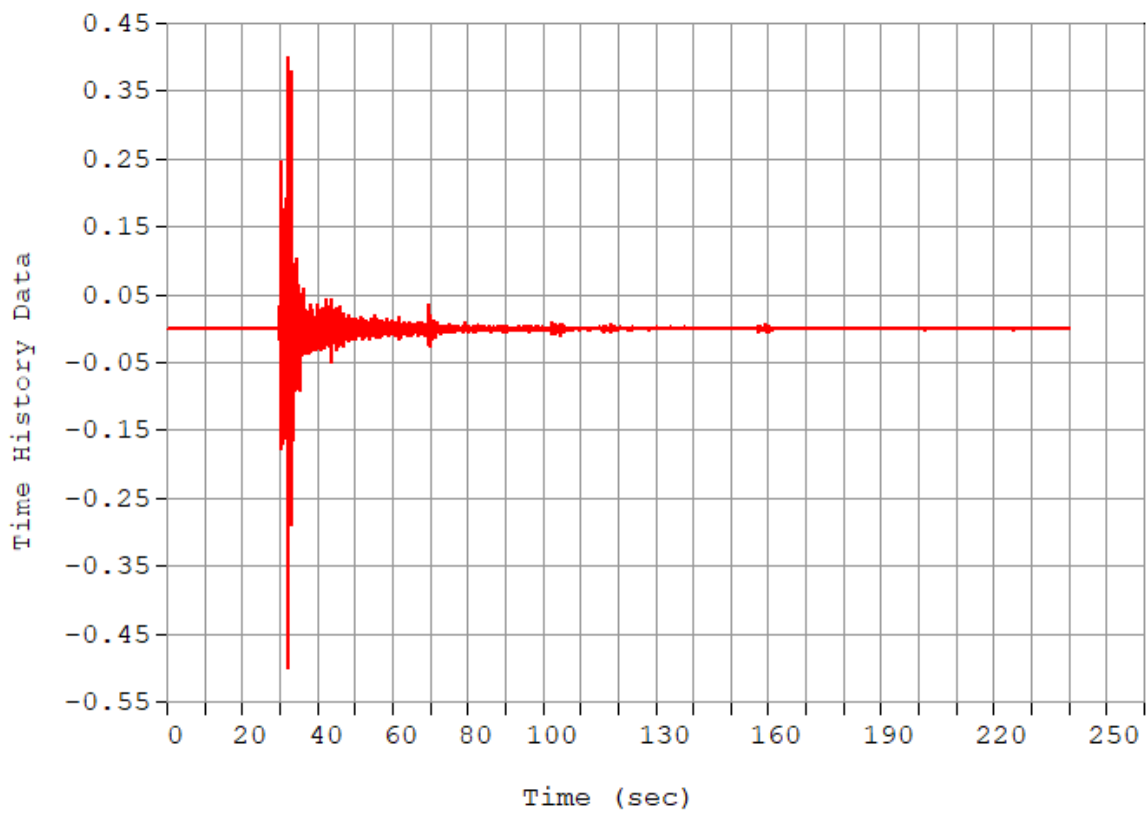


Figure 38 GM1 THA 0.5g

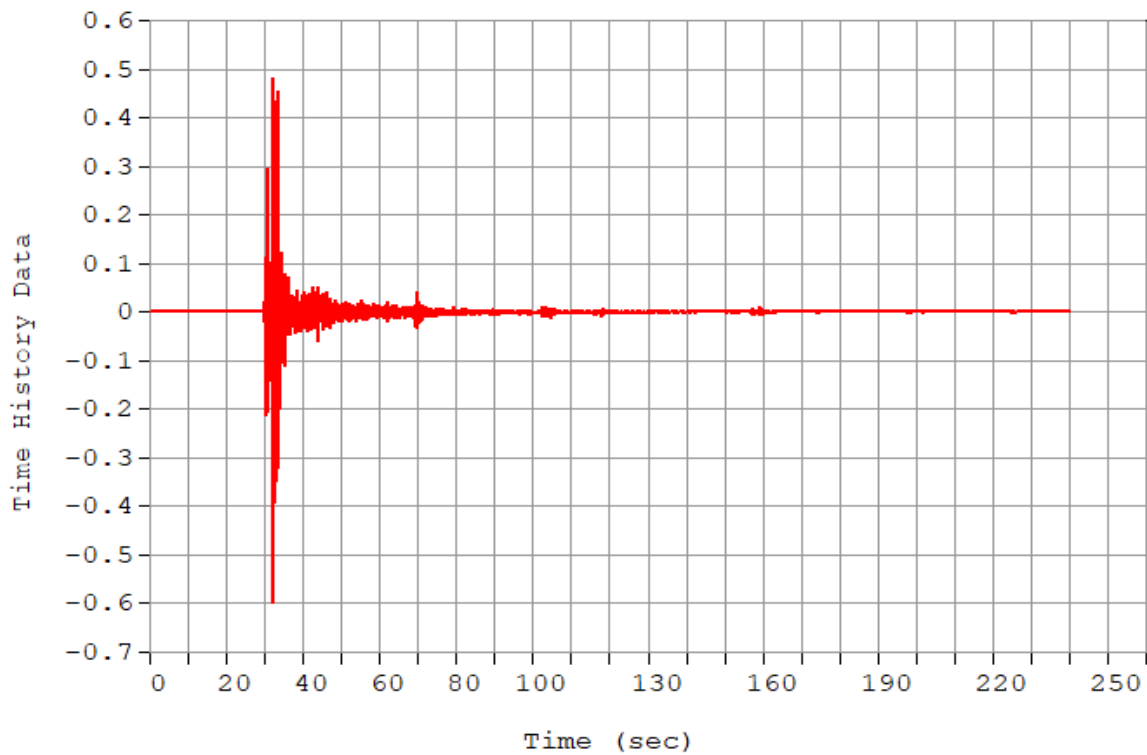


Figure 37 GM1 THA 0.6g

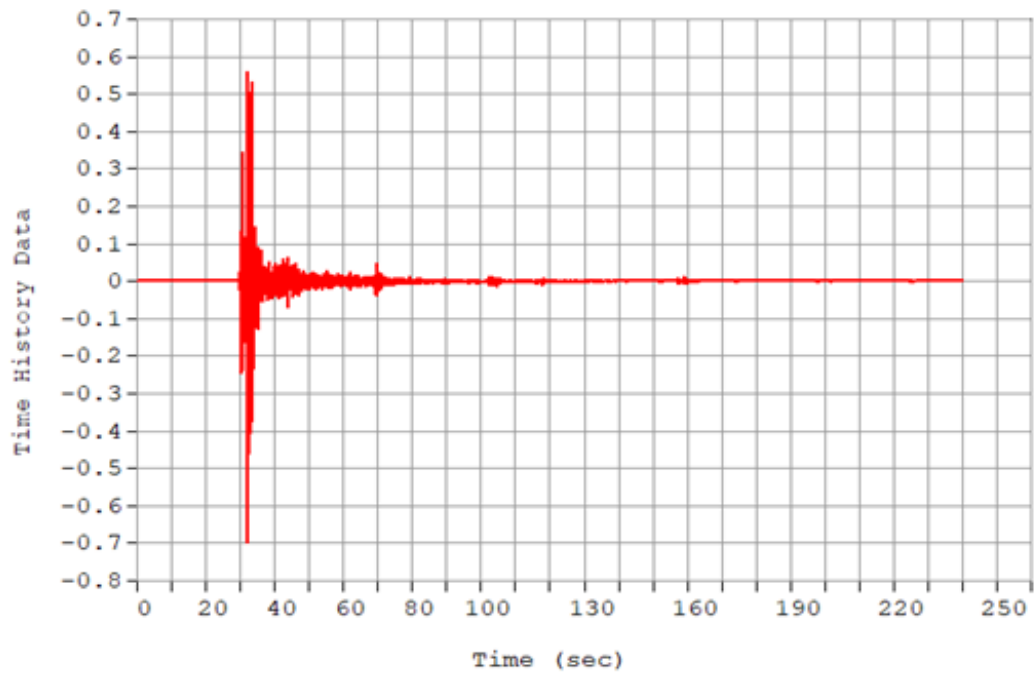


Figure 40 GM1 THA 0.7g

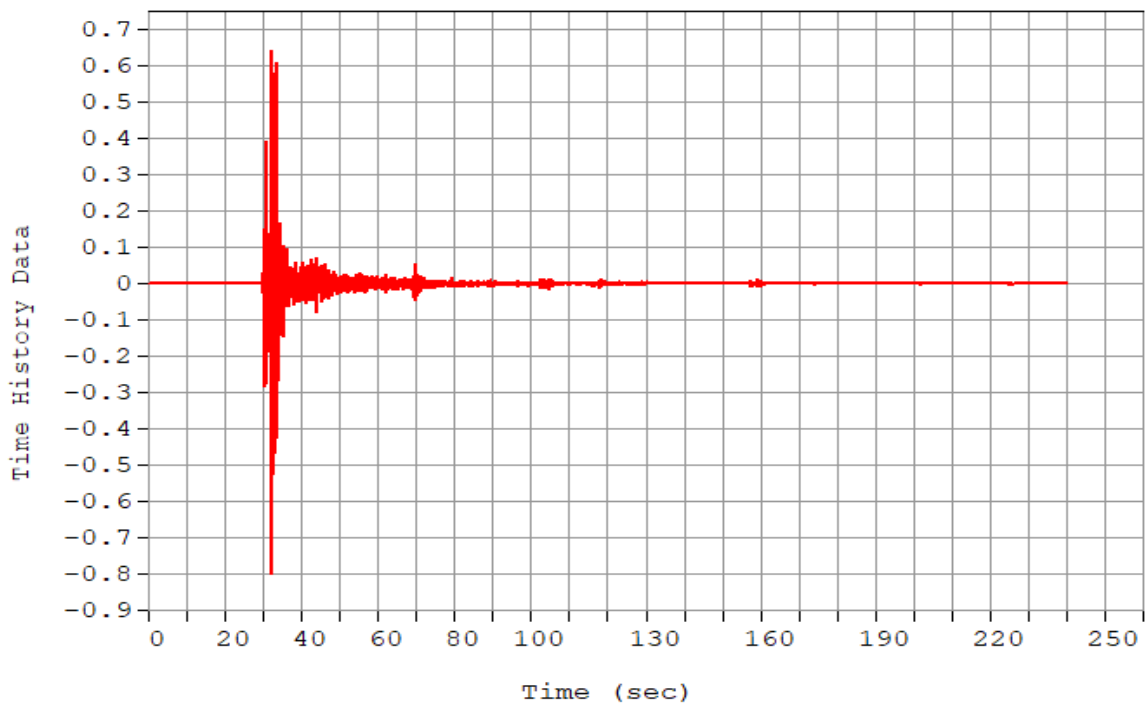


Figure 39 GM1 THA 0.8g

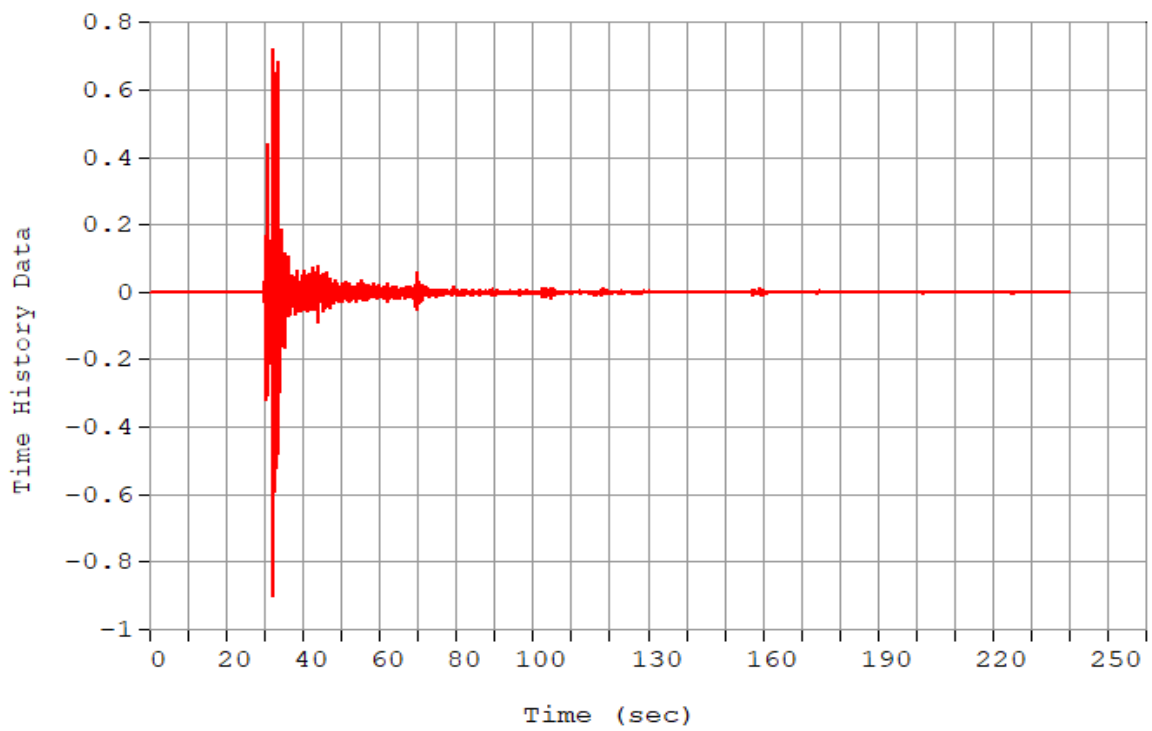


Figure 42 GM1 THA 0.9g

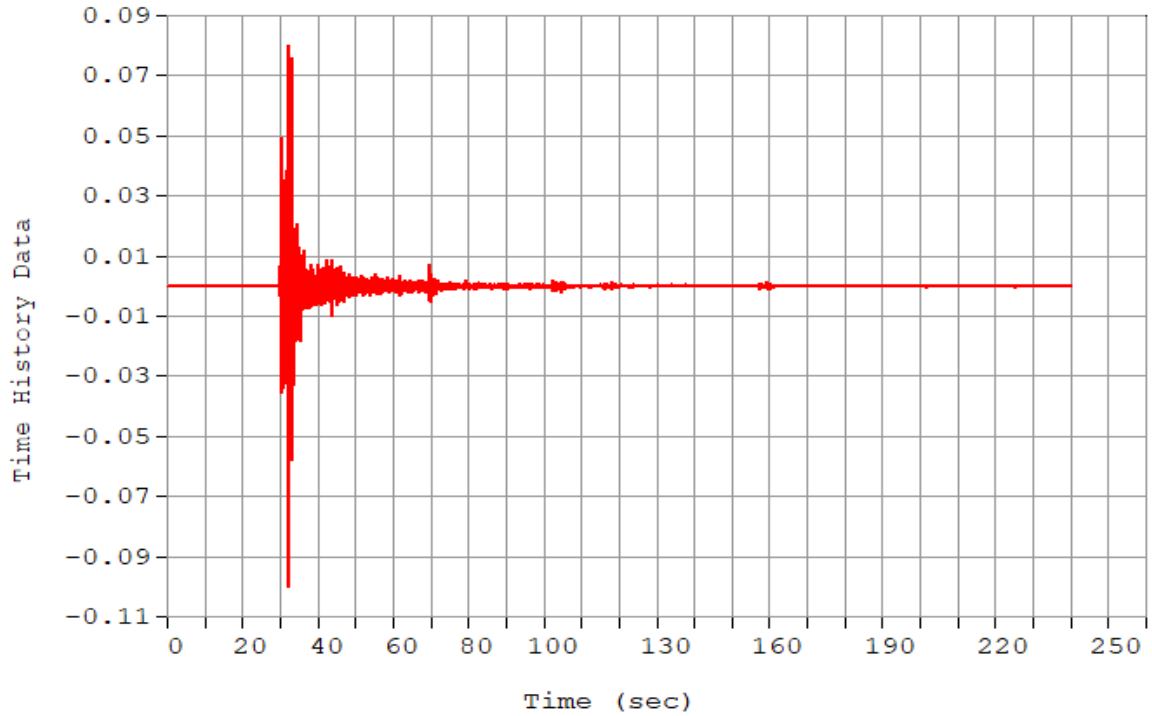


Figure 41 GM1 THA 1g

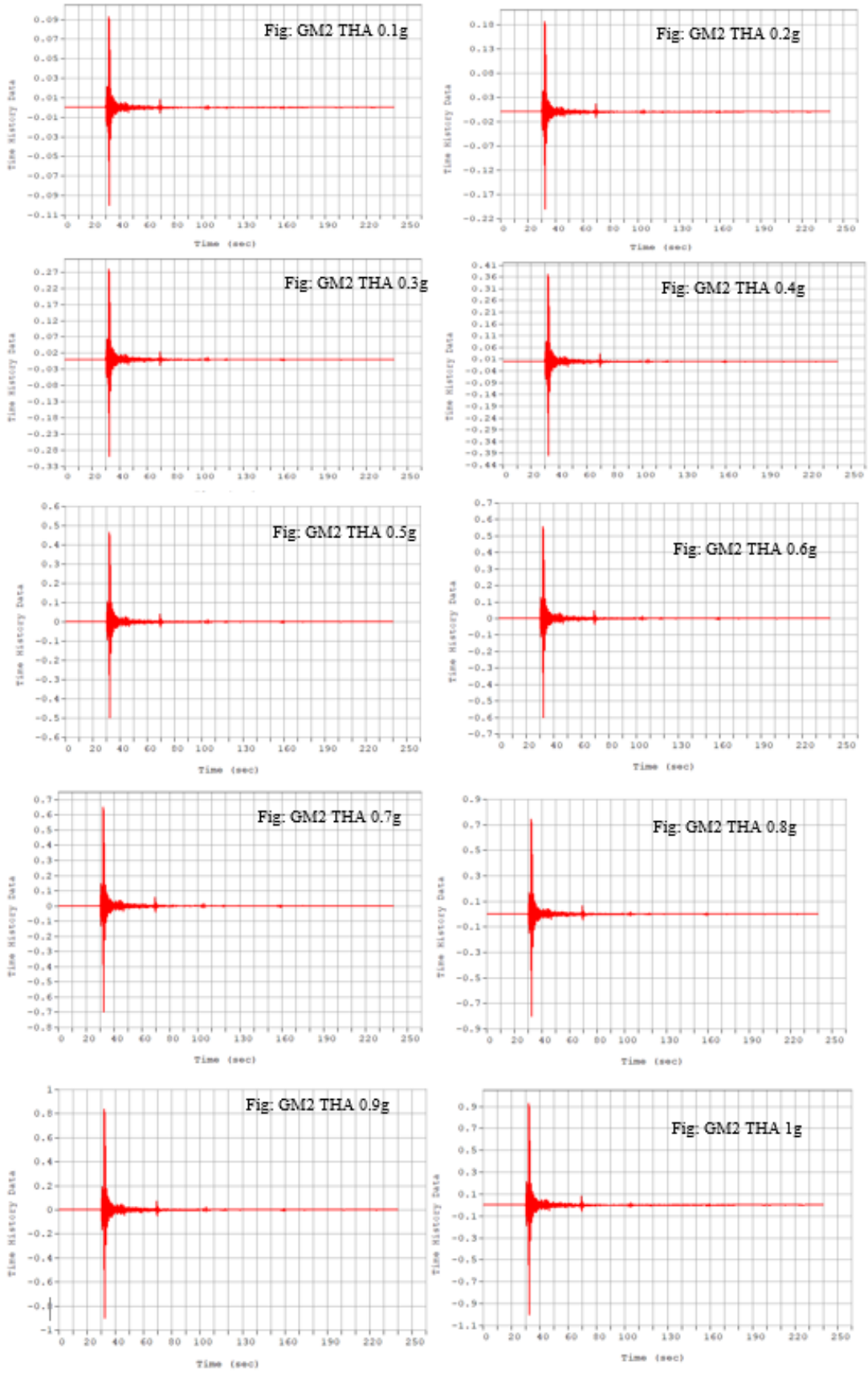


Figure 43 GM2 THA 0.1g to GM2 THA 1g

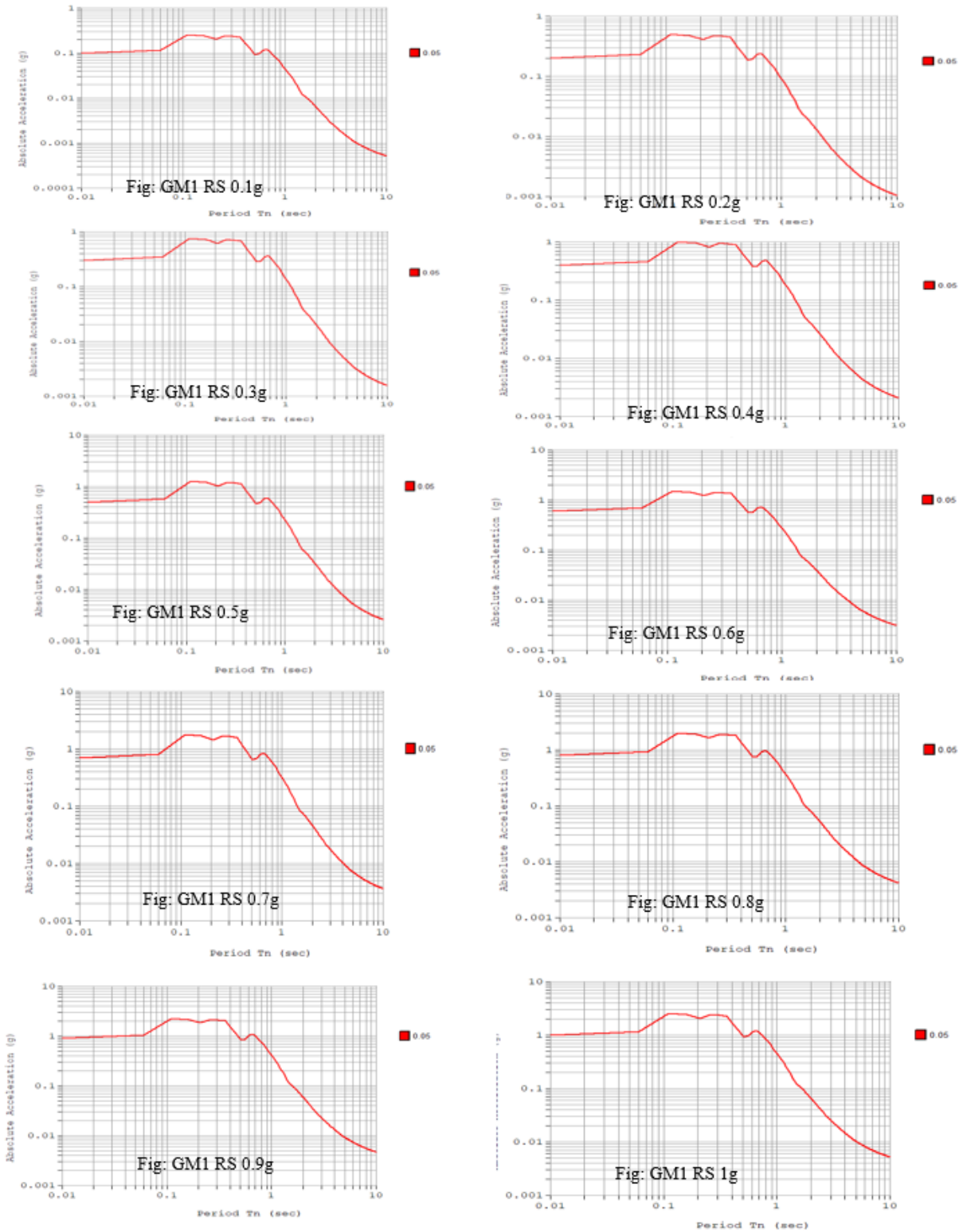


Figure 44 GM1 Response Spectrum

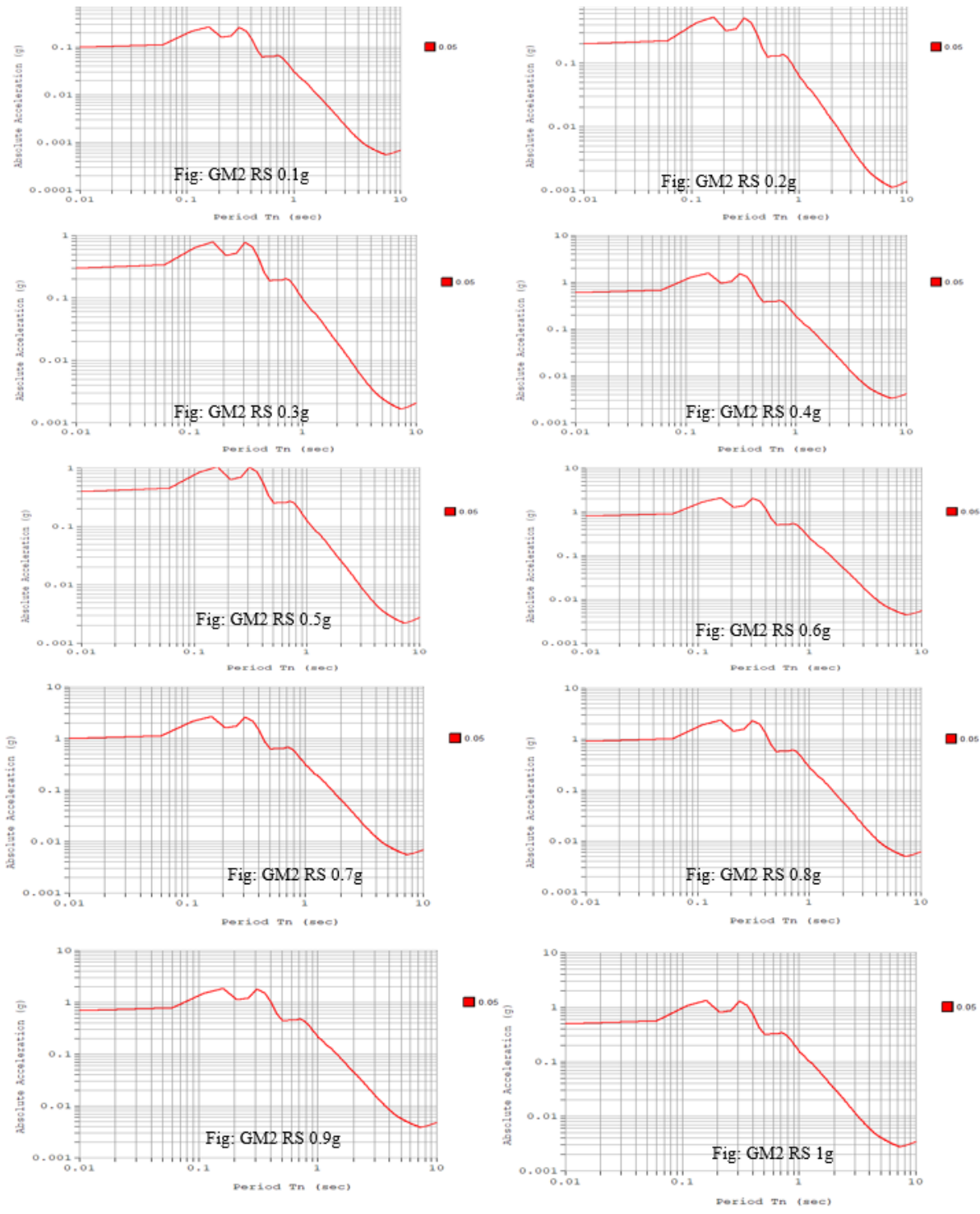


Figure 45 GM2 Response Spectrum

Next add time history load case and the method of analysis.

- Modal analysis is a method used in engineering to examine a structure or system's dynamic behaviour. It entails identifying and characterising the natural vibrational modes, frequencies, and associated modal parameters

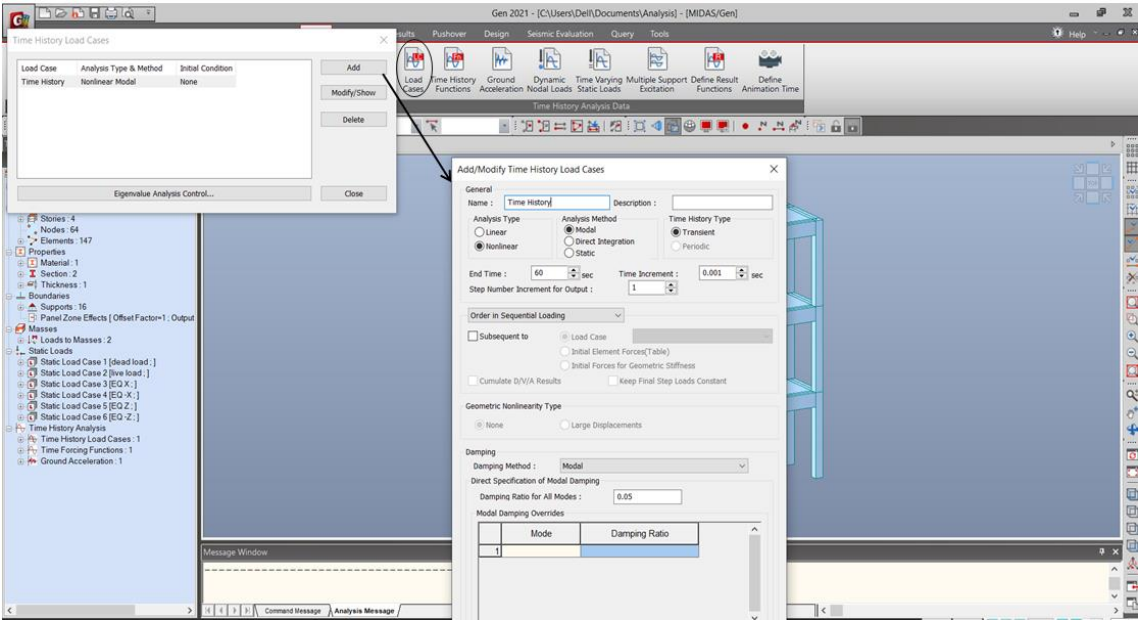


Figure 46 Adding Time History load case

Add the ground acceleration data like arrival time and scale factor in each direction.

- Arrival time is the time at which load assignment begins during analysis.it is being taken as 0.001sec
- Scale factor is the coefficient multiplied with the load during analysis. Here it is taken as 1.

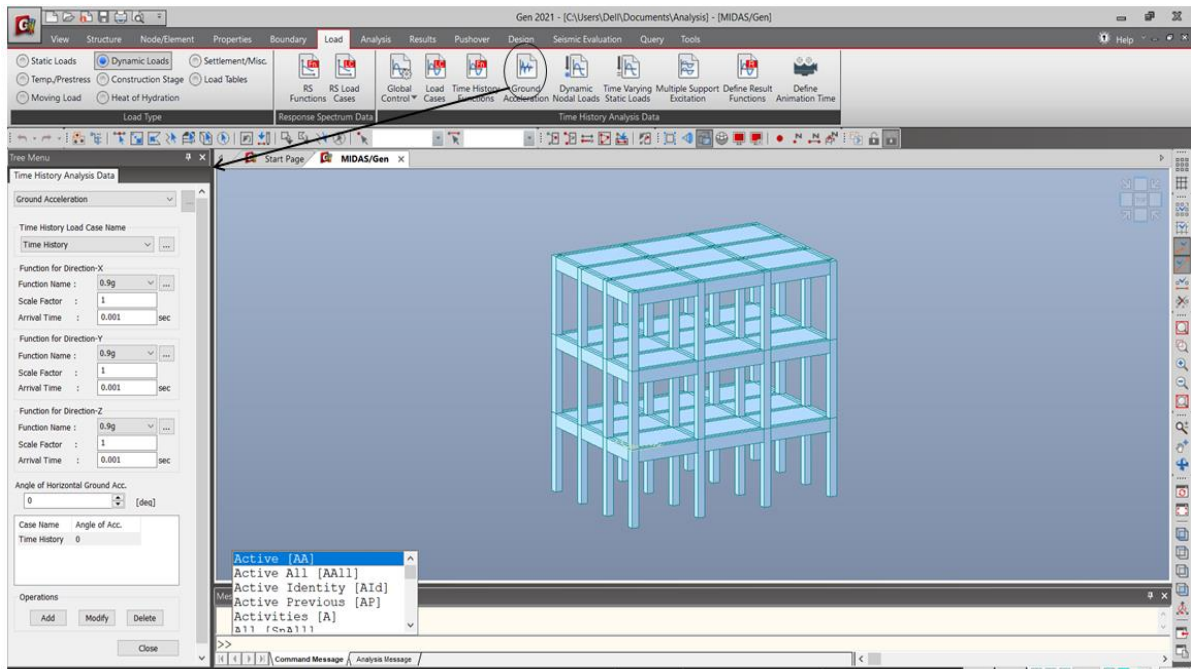


Figure 47 Adding ground acceleration data like arrival time and scale factor in each direction

Finally perform the analysis

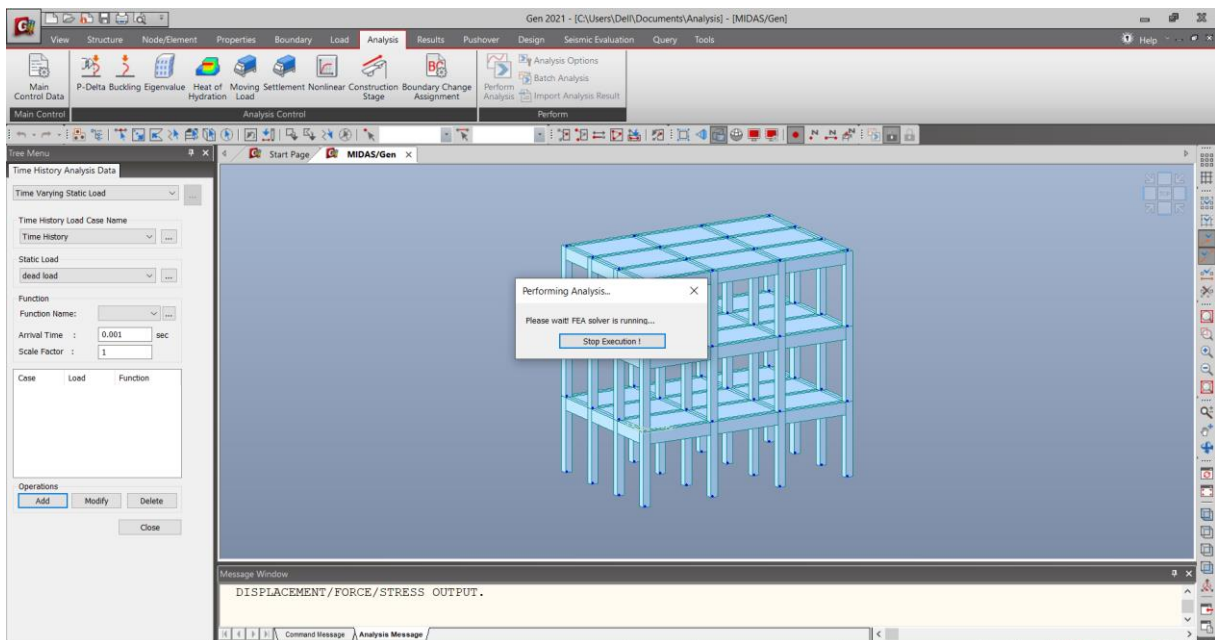


Figure 48 Performing Analysis

3. Result

From the result extract the inter story drift due to time history load.

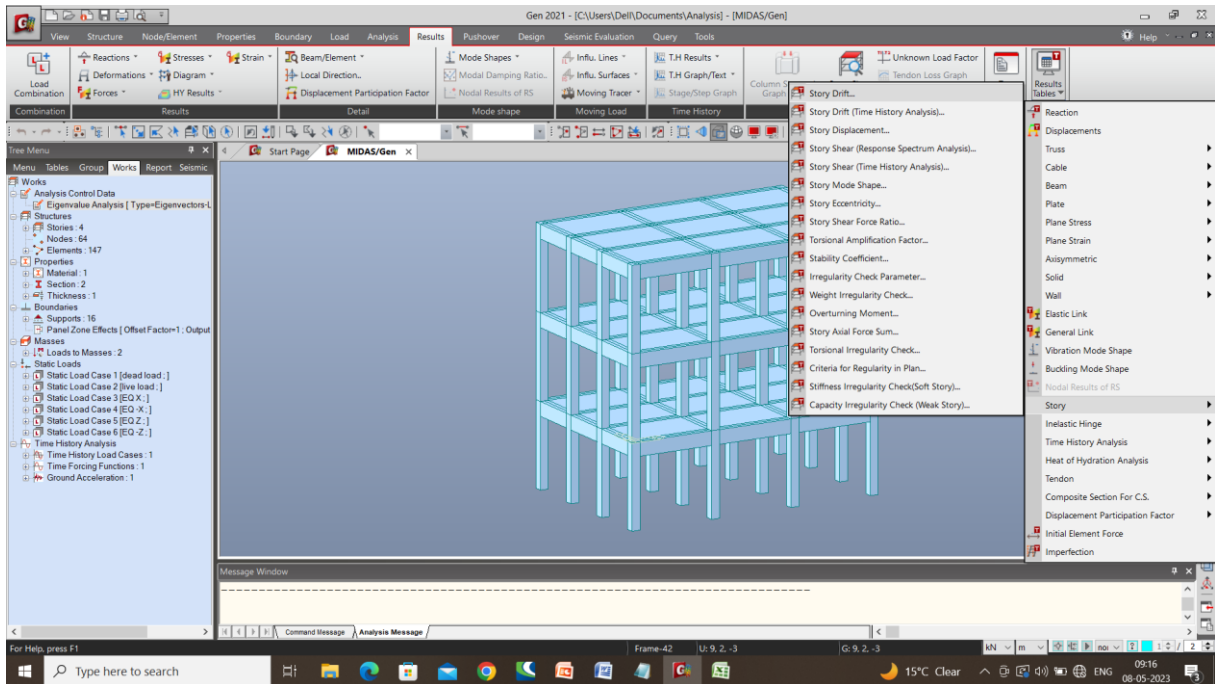


Figure 49 Result

Apply the dead load and live load scale factor

- The drift movable factor is taken as 0.004
- The live load scale factor for building storey up to and including 3rd floor is taken as 25%.

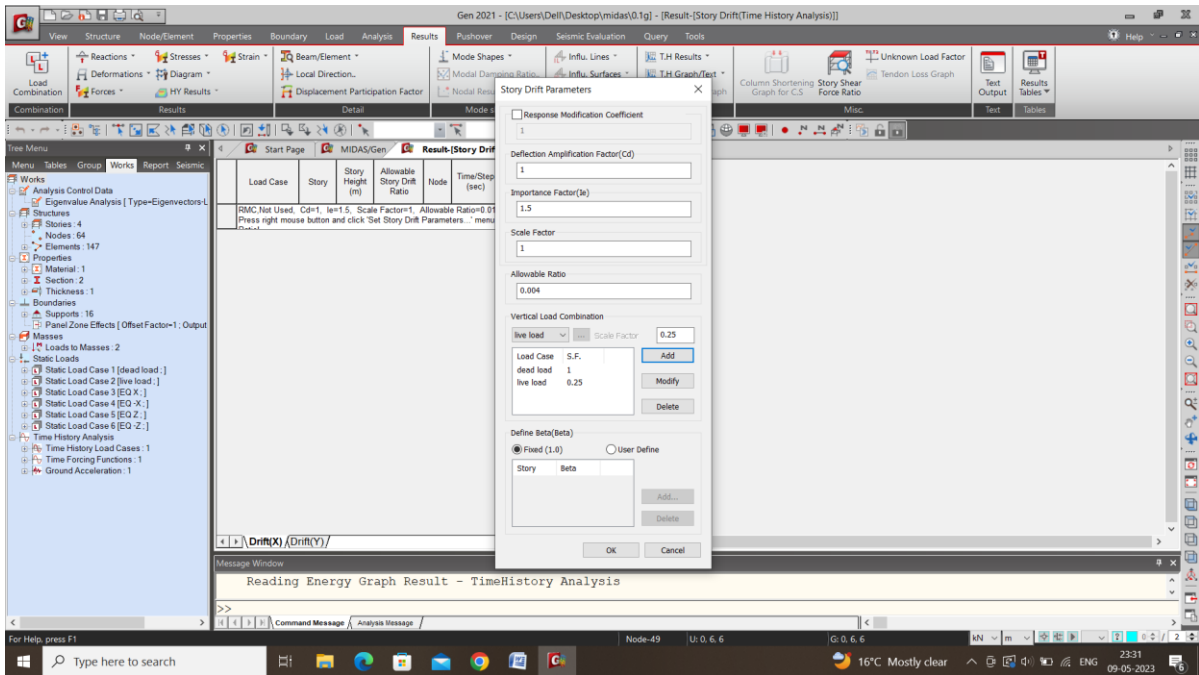


Figure 50 Applying the dead load and live load scale factor

Similarly extract the results from other spectral acceleration data.

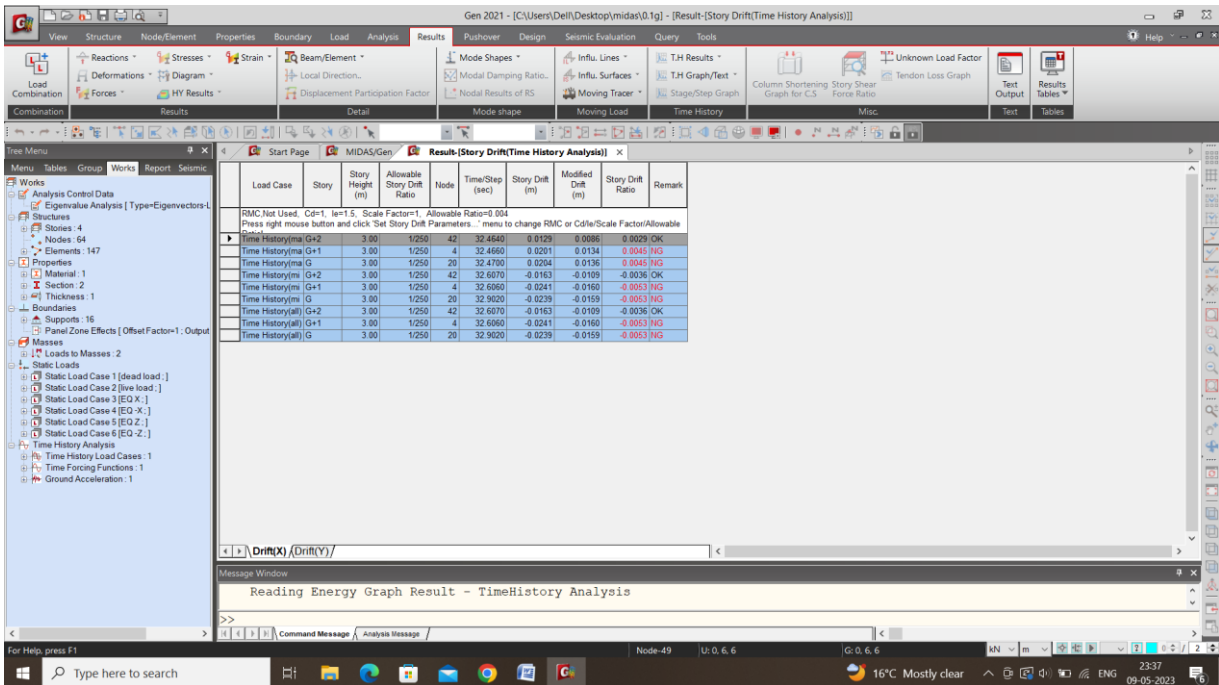


Figure 51 Extracting the Results from other spectral Acceleration Data

Analyse the drift result

- Check which storey failed under which load and analyse the result.

SA (g)		0.1g			0.2g			0.3g			0.4g			0.5g		
Storey		G	G+1	G+2	G	G+1	G+2	G	G+1	G+2	G	G+1	G+2	G	G+1	G+2
Drift (m)	GM1	-0.0024	-0.0024	-0.0016	-0.0048	-0.0048	-0.0033	-0.0072	-0.0072	-0.0049	-0.0096	-0.0096	-0.0065	-0.012	-0.012	-0.0082
		Safe	Safe	Safe	Safe	Safe	Safe	Safe	Safe	Safe	Safe	Safe	Safe	Safe	Safe	Safe
	GM2	0.0026	-0.0024	-0.0015	0.0051	-0.0048	-0.003	0.0077	-0.0072	-0.0045	0.0103	-0.0096	-0.006	0.0128	-0.012	-0.0075
		Safe	Safe	Safe	Safe	Safe	Safe	Safe	Safe	Safe	Safe	Safe	Safe	Safe	Safe	Safe

SA (g)		0.6g			0.7g			0.8g			0.9g			1g		
Storey		G	G+1	G+2	G	G+1	G+2	G	G+1	G+2	G	G+1	G+2	G	G+1	G+2
Drift (m)	GM1	-0.0143	-0.0144	-0.0098	-0.0167	-0.0168	-0.0114	-0.0191	-0.0192	-0.013	-0.0215	-0.0216	-0.0147	-0.0239	-0.0241	-0.0163
		Safe	Safe	Safe	Fail	Fail	Safe	Fail	Fail	Safe	Fail	Fail	Safe	Fail	Fail	Safe
	GM2	0.0154	-0.0144	-0.009	0.018	-0.0168	-0.0105	0.0205	-0.0191	-0.012	0.0231	-0.0215	-0.0135	0.0257	-0.0239	-0.015
		Safe	Safe	Safe	Safe	Safe	Safe	Fail	Fail	Safe	Fail	Fail	Safe	Fail	Fail	Safe

Figure 52 Analysing Drift Result

SA (g)	No. of storeys failed	
	GM1	GM2
0.1g	0	0
0.2g	0	0
0.3g	0	0
0.4g	0	0
0.5g	0	0
0.6g	0	0
0.7g	2	0
0.8g	2	2
0.9g	2	2
1g	2	2

GM1: According to the analysis result, the building started to fail when 0.6g spectral data was being applied and completely failed upon applying spectral data above 0.6g.

GM2: According to the analysis result, the building started to fail when 0.7g spectral data was being applied and completely failed upon applying spectral data above 0.8g.

Figure 53 Drift Result

2. Analyse the result.

The storey displacement when subjected to the spectral acceleration which led to failure of the model.

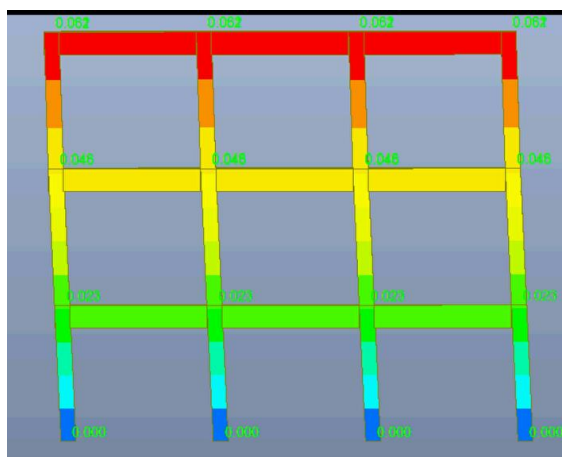


Figure 54 GM2: at 0.8g, G and G+1 storey failed.

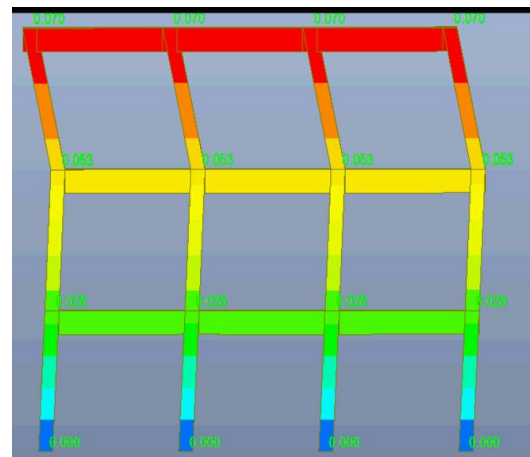


Figure 55 GM1: at 0.7g, G and G+1 storey failed.

After analysing the inter storey drift result, according plot the fragility curve.

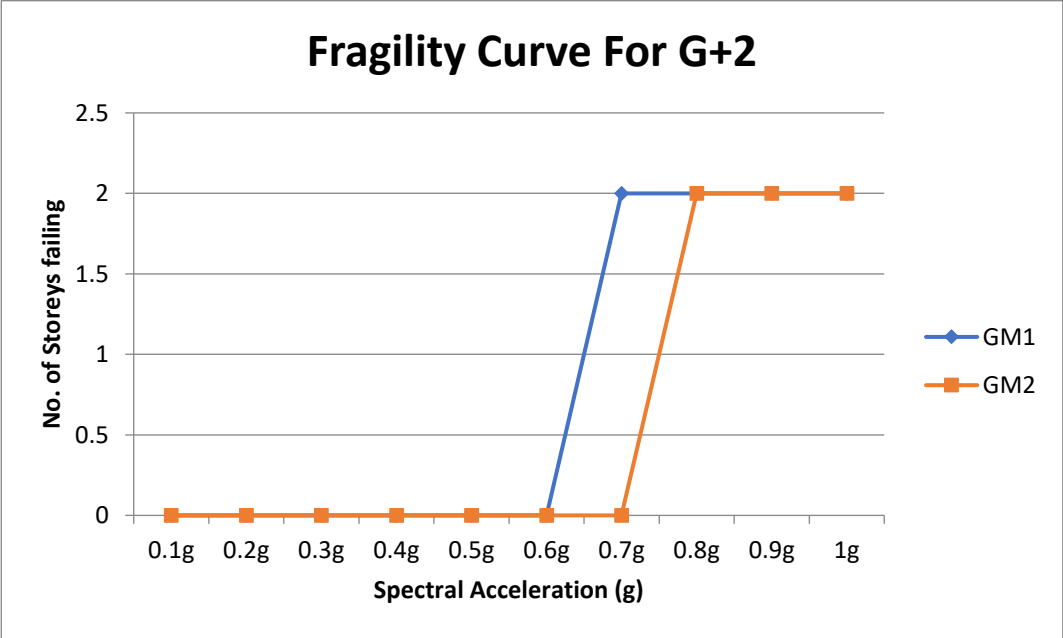


Figure 56 Fragility Curve for G+2

From the curve, it can be said that the probability of failure of the model building is comparatively less and the damage sustained by the beams and columns is slight to moderate. It can be observed that the building fails only at higher ground acceleration, which in reality does not occur much often, so the design can be considered uneconomical. It can also be concluded that the design turned out to be more toward the target of earthquake proof rather than earthquake resistant which is expensive and unnecessary.

CHAPTER 6

CONCLUSION & RECOMMENDATIONS

Conclusion

After a significant earthquake, it is clear that hospitals must be operational. This is rarely contested. While it is common practice to complement destroyed hospitals with emergency field hospitals, medical tents and air-lifts to nearby institutions, they are never a suitable replacement. Even though the measures are being taken every now and then to prevent devastating casualties of earthquake, the infrastructures are difficult to be earthquake proof so rather it is designed in such a way that it can at least withstand certain intensities.

Non-structural components safety is difficult to analyze as there are no software or proven procedures to do. It can be mainly done by studying published literatures and researches done by the experts in the field. It can be concluded that as long as all the codal provisions are being followed while installing the non-structural component, less to no damage will be sustained the components.

Structural components of a hospital are like the spine of the body. They should be all properly designed for the hospital to function properly pre and post-earthquake. From the analysis result, it can be concluded that the model hospital can withstand up to certain standard earthquake intensities and might function to its full ability post-earthquake. The design seems economical as it is cordially accepted when a structural components fails on and after application of spectral acceleration after 0.5g. Since the model starts to fail only after 0.7g it can be said that the model is earthquake resistant.

Recommendations

It is advisable to consider incorporating non-structural components such as piping and electrical equipment systems into advanced software like SAP when modeling structures, in order to achieve more practical and realistic results.

To analyze the impact of torsion, it is recommended to use ground motion data in two directions. Furthermore, when constructing building models, it would be beneficial to include structural walls and analyze their response to subjected ground motion.

REFERENCES

- [1] Arnold,C., and Reitherman,R., (1982), *Building Configuration and Seismic Design*, JohnWiley, USA
- [2] Lagorio,H,J, (1990), *EARTHQUAKES An Architect's Guide to Non-Structural Seismic Hazard*, John Wiley & Sons, Inc., USA.
- [3] *Hazard*, John Wiley & Sons, Inc., USA.
- [4] Kramer, S., (2014) “Geotechnical earthquake engineering,” *Noida: Pearson India Education Services*.<https://www.nicee.org/EQTips.php>
- [5] Baker, J., Bradley, B. and Stafford, P., n.d. *Probabilistic seismic hazard and risk analysis*.
- [6] Takeuhi, H., and Fumiko, C., (1971) “The Elastic Rebound Theory and The Mantle Convection,” *Zisin (Journal of the Seismological Society of Japan, 2nd Ser.)*, Vol. 24, No. 2, pp. 162–64, DOI: https://doi.org/10.4294/zisin1948.24.2_162.
- [7] Balkema (1999) “1: Keynote Lectures, Theory of Vibration, Stochastic Dynamics, Non – Linear Vibration, Vibration of Structural Elements, Wave Propagation, Material Properties and Noise, Experimental Methods in Dynamics,” *Structural Dynamics*.
- [8] Abrahamson N, Gregor N, Addo K (2016) *BC hydro ground motion prediction equations for subduction earthquakes*. *Earthq Spectra* 32(1):23-44. <https://doi.org/10.1193/051712EQS188MR>
- [9] Asimaki D et al (2017) *Observations and simulations of basin effects in the Kathmandu valley during the 2015 Gorkha, Nepal, earthquake sequence*. *Earthq Spectra* 33(S1):S35–S53. <https://doi.org/10.1193/013117EQS022M>
- [10] Ares, A. F., &Fatehi, A. (2013). Development of probabilistic seismic hazard analysis for international sites, challenges and guidelines. *Nuclear Engineering and Design*, 259, 222–229. <https://doi.org/10.1016/j.nucengdes.2011.01.024>
- [11] Stevens, V. L., De Risi, R., Roux-Mallouf, R. L., Drukpa, D., &Hetényi, G. (2020). *Seismic hazard and risk in Bhutan*. *Natural Hazards*, 104(3), 2339–2367. <https://doi.org/10.1007/s11069-020-04275-3>
- [12] Sianko, I., Ozdemir, Z., Khoshkholghi, S., Garcia, R., Hajirasouliha, I., Yazgan, U., &Pilakoutas, K. (2020). A practical probabilistic earthquake hazard

analysis tool: case study Marmara region. *Bulletin of Earthquake Engineering*, 18(6), 2523–2555. <https://doi.org/10.1007/s10518-020-00793-4>

- [13] Cornell, C. A. (1968). *Engineering seismic risk analysis*. Bulletin of the Seismological Society of America, 58(5), 1583-1606.
- [14] McGuire, R. K. (1976). *Fortran computer program for seismic risk analysis*. US Geological Survey, Open-File Report 76-67.
- [15] Baker, J. W. (2011). *Conditional mean spectrum: Tool for ground-motion selection*. Journal of Structural Engineering, 137(3), 243-251.
- [16] Pezeshk, S., Hamburger, R. O., & Moehle, J. P. (2011). *The role of epistemic uncertainty in seismic hazard analysis*. Earthquake Engineering & Structural Dynamics, 40(7), 809-826.
- [17] Abrahamson, N. A., & Silva, W. J. (2008). *Summary of the ASK14 ground motion relation for active crustal regions*. Earthquake Spectra, 24(1), 67-97.
- [18] Danciu, L., & Giardini, D. (2012). *Seismic hazard assessment: the state-of-the-art in Europe*. Soil Dynamics and Earthquake Engineering, 32, 54-68.
- [19] Edwards, B., & Yeo, E. T. (2012). *A comprehensive review of probabilistic seismic hazard analysis (PSHA): methods, challenges and opportunities*. Tunnelling and Underground Space Technology, 27, 94-109.
- [20] Jayaram, N., & Baker, J. W. (2009). *Bayesian model selection for ground motion prediction equations in probabilistic seismic hazard analysis*. Earthquake Spectra, 25(3), 543-560.
- [21] Ordaz, M., & Iervolino, I. (2016). *A comparison of alternative methods for spatially correlated ground motion fields in probabilistic seismic hazard analysis*. Bulletin of Earthquake Engineering, 14(3), 863-888.

JAYPEE UNIVERSITY OF INFORMATION TECHNOLOGY, WAKNAGHAT
PLAGIARISM VERIFICATION REPORT

Date:

Type of Document (Tick): PhD Thesis M.Tech Dissertation/ Report B.Tech Project Report Paper

Name: _____ Department: _____ Enrolment No _____

Contact No. _____ E-mail. _____

Name of the Supervisor: _____

Title of the Thesis/Dissertation/Project Report/Paper (In Capital letters): _____

UNDERTAKING

I undertake that I am aware of the plagiarism related norms/ regulations, if I found guilty of any plagiarism and copyright violations in the above thesis/report even after award of degree, the University reserves the rights to withdraw/revoke my degree/report. Kindly allow me to avail Plagiarism verification report for the document mentioned above.

Complete Thesis/Report Pages Detail:

- Total No. of Pages =
- Total No. of Preliminary pages =
- Total No. of pages accommodate bibliography/references =

(Signature of Student)

FOR DEPARTMENT USE

We have checked the thesis/report as per norms and found **Similarity Index** at(%). Therefore, we are forwarding the complete thesis/report for final plagiarism check. The plagiarism verification report may be handed over to the candidate.

(Signature of Guide/Supervisor)

Signature of HOD

FOR LRC USE

The above document was scanned for plagiarism check. The outcome of the same is reported below:

Copy Received on	Excluded	Similarity Index (%)	Generated Plagiarism Report Details (Title, Abstract & Chapters)	
	<ul style="list-style-type: none"> • All Preliminary Pages • Bibliography/Images/Quotes • 14 Words String 		Word Counts	
Report Generated on			Character Counts	
		Submission ID	Total Pages Scanned	
			File Size	

Checked by
Name & Signature

Librarian

Please send your complete thesis/report in (PDF) with Title Page, Abstract and Chapters in (Word File) through the supervisor at plagcheck.juit@gmail.com